Geochimica et Cosmochimica Acta 359 (2023) 176–190

Contents lists available at ScienceDirect

Geochimica et Cosmochimica Acta

journal homepage: www.elsevier.com/locate/gca

Deposition of Mo, Re and U under contrasting redox conditions; assessment of the $[Re/Mo]_{sw}$ redox proxy

I. Živković [a,c], E. Bura-Nakić [a], L. Knežević [a], G.R. Helz [b,*]

[a] Division for Marine and Environmental Research, Rudjer Bošković Institute, Bijenička cesta 54, 10000 Zagreb, Croatia
[b] Department of Chemistry and Biochemistry and Department of Geology, University of Maryland, College Park MD 20746, USA
[c] Department of Environmental Sciences, Jožef Stefan Institute, Jamova cesta 39, 1000 Ljubljana, Slovenia

ARTICLE INFO

Associate editor: Susan Halsall Little

Keywords:
Redox proxies
Meromictic lakes
Molybdenum
Rhenium
Uranium

ABSTRACT

We have analyzed concentrations of Mo, Re and U in the suspended particles, water column, underlying carbonate-dominated sediments and pore waters of two contrasting marine lakes situated on the Adriatic Coast of Croatia. Our data are the first for Re in these lakes. Rogoznica Lake is mainly euxinic, but subject to occasional oxygenation events, whereas Mljet Island's Malo Jezero is currently oxic year around but historically was seasonally euxinic. These characteristics make the lakes useful testing grounds for redox proxies. We devote particular attention to Re/Mo ratios, which have great promise as redox proxies. In marine sediments, the range of $\log[Re_{auth}/Mo_{auth}]$ exceeds 2, and typical analytical uncertainty is ±0.05, providing resolving power similar to δ^{98}Mo. Authigenic $[Re_s/Mo_s]$ ratios in sediments depend on varying supplies of three components: $FeMo,Re)S_4$ coprecipitates, Fe(III) oxyhydroxides (plus Mn(III,IV) oxyhydroxides in some cases) and a still-uncharacterized Re-rich, Mo-poor component possibly of biological origin. Removal of the latter component explains a 50% depletion of Re_{aq} without Mo_{aq} from Rogoznica's oxic waters. Water column concentrations of Mo_{aq} and Re_{aq}, as well as $[Re_s/Mo_s]$ ratios in Rogoznica's suspended particles are predicted successfully by a model that attributes these elements' removal from sulfidic seawater solely to coprecipitation in $Fe(Mo,Re)S_4$, assuming a partition coefficient of 0.6. However, to predict sediment compositions, additional authigenic Mo supplied by mainly Fe (III) oxyhydroxides during sporadic oxygenation events must be considered. In Malo Jezero, sulfide concentrations are too low even in pore waters for precipitation of $Fe(Mo,Re)S_4$. Consistent with earlier work, U_{aq} profiles are best explained by eddy diffusive transport to the sediment rather than capture by a precipitate in the water column. In Rogoznica pore waters, Mo_{aq} extracted through 0.45 μm pore size filters exceeds by 50-fold concentrations predicted by the model and measured previously with 0.15 μm filters. This observation implies presence of ferrothiomolybdate colloids, which could be important, overlooked participants in the sedimentary geochemistry of Mo.

1. Introduction

In oxic and in anoxic but non-sulfidic marine water columns, dissolved concentrations of Mo, Re and U are nearly constant vertically (Anbar et al. (1992; Nameroff et al., 2002; Singh et al., 2011; Goswami et al., 2012, 2022; Ho et al., 2018; Dickson et al., 2020), implying that neither abiotic nor biotic scavenging or precipitation occurs to a meaningful extent. In contrast, dissolved forms of all three elements become depleted in significantly sulfidic water columns or pore waters, and associated sediments become enriched (Emerson and Huested, 1991; Colodner et al., 1995; Morford et al., 2005, 2007, 2012; Rolison et al., 2017). These elements' enrichments in sedimentary rocks are therefore interpreted as proxies that indicate sulfidic conditions during those rocks' deposition.

Importantly, depletions of Mo_{aq} and Re_{aq} under sulfidic conditions never reach analytical detection limits. Mo_{aq} declines to pH-sensitive, sulfide-independent solubility minima, causing aqueous concentrations to approach asymptotes. The asymptotes are independent of organic carbon availability, proving that the so-called organic pathway for Mo_{aq} removal from euxinic natural waters is unimportant in nature (Helz, 2021). By preventing quantitative scavenging of Mo_{aq} and requiring a small degree of Mo_{aq} return to the ocean, solubility

* Corresponding author.
E-mail address: helz@umd.edu (G.R. Helz).

https://doi.org/10.1016/j.gca.2023.08.020
Received 24 April 2023; Accepted 22 August 2023
Available online 25 August 2023

asymptotes hinder sediments from fully acquiring seawater's $\delta^{98}Mo$ signature (Helz, 2021). The Mo_{aq} asymptotes have been attributed to the equilibrium solubility of $FeMoS_4$ (Vorlicek et al., 2018; Helz and Vorlicek, 2019), and the Re_{aq} limits may reflect Re_{aq} control by coprecipitation with $FeMoS_4$ (Helz and Dolor, 2012; Helz, 2022). Morford et al. (2005) propose that U^{VI}_{aq}, which can be a terminal electron acceptor in microbial metabolism, is alternatively limited to the minimum concentration capable of supplying biologically useful energy.

Early researchers assumed that these elements' authigenic enrichment mechanisms simply involved reduction of seawater's MoO_4^{2-}, $UO_2(CO_3)_n^{+2-2n}$ or ReO_4^- to tetravalent oxides or other unspecified reduction products (Piper and Isaacs, 1995; Crusius et al., 1996). Also, capture of these elements by unspecified organic functional groups was often proposed (reviewed by Smedley and Kinniburgh, 2017; Helz and Vorlicek, 2019; Phillips and Xu, 2021). Ambiguities about these mechanisms have impeded rigorous testing. However, as methods such as x-ray spectroscopy evolved for studying chemical properties of sub-micron and amorphous forms of trace elements in sediments, these concepts proved overly simplistic. In the case of uranium, the tetravalent oxide (UO_2, uraninite) indeed is common in sediments and soils, but both U^{VI} and U^{IV} organic complexes as well as U^{VI} carbonates, silicates and phosphates are also found (Jerden and Sinha, 2003; Sharp et al., 2011; Mikutta et al., 2016; Smrzla et al., 2019; Bone et al., 2020; Fuller et al., 2020). In the case of molybdenum, MoO_2 is too soluble to appear in sediments. Beneath euxinic Lake Cadagno, x-ray spectra reveal one form in which Mo has mixed O- and S-coordination with a mean oxidation state of +5.3 to +5.5 and another form in which Mo is predominantly S-coordinated with a mean oxidation state of +4.4 to +4.5 (Dahl et al., 2013). The form of Re in natural sediments has not yet been observable owing to its low concentrations. However, Yamashita et al. (2007) injected sufficient ReO_4^- into biologically active, reducing sediments to produce interpretable x-ray spectra; these revealed changes explainable by incomplete reduction or by Re thiolation ($ReO_4^- \rightarrow ReS_4^-$).

The plan for this paper is to examine the scavenging and deposition patterns of Mo, Re and U in two marine lakes. The lakes are similar in most respects, including extremely restricted exchange with the surrounding sea, but differ in their dominant water column redox characteristics, one being oxic and the other euxinic. Previously Mo and U, as well as their isotopes, have been discussed in these lakes (Helz et al., 2011a; Bura-Nakić et al., 2018, 2020). Our focus here is not on the lakes themselves but on what they can teach about the mechanisms that control the behavior of redox sensitive elements.

2. Methods

2.1. Locality description

Rogoznica Lake (locally known as Zmajevo Oko, Dragon's Eye Lake; 43°31.8′N 15°57.5′E) is located on a small peninsula protruding into the Adriatic Sea from the west coast of Croatia. Malo Jezero (Small Lake; 42°47′N 17°21′E) is located 150 km to the southeast from Rogoznica Lake on the Croatian island of Mljet. Both are situated in lithologically simple drainage basins consisting only of limestone with minor dolomite. Malo Jezero sediments are aragonite-dominated with total $CaCO_3$ reaching 72%, whereas Rogoznica Lake sediments are calcite-dominated with total $CaCO_3$ up to 92% (Mihelčić et al., 1996; Sondi and Juračić, 2010; Sondi et al., 2017).

The terrane began in the Mesozoic as a Bahamas-like platform that accumulated carbonate sediments to a thickness of >5 km. Tectonic deformation, beginning in the late Cretaceous and climaxing in the Oligocene/Miocene, thrust up the limestones and dolomites forming the Dinaric Alps (Vlahović et al., 2005). This karstified, mountainous terrain now buttresses the Adriatic coast of the Balkan Peninsula. When sea-level dropped during the Pleistocene, caves and dolines (topographic basins that lack surface outlets and drain through karst) penetrated the limestone and dolomite to depths below modern sea-level. Subsequently, rising sealevel has drowned these features (Surić et al., 2005; Razum et al., 2021), converting the dolines and exposed caves into the conspicuous marine lakes and embayments that adorn the Adriatic coast today.

Both lakes experience a Mediterranean climate with annual precipitation of ≈1 m/yr, two-thirds arriving between October and March. Potential evaporation considerably exceeds precipitation, so very little precipitation reaches the lakes as surface runoff, but subaquatic, freshwater springs are known (Wunsam et al., 1999; Cuculić et al., 2009). Rogoznica Lake has no surface inlet or outlet to the Adriatic Sea but weak tides reveal subterranean connections. Malo Jezero has only a narrow opening (≈2 m^2 cross section) to an adjacent marine lake (Veliko Jezero) that in turn connects to the Adriatic Sea. Both can be described as highly restricted basins. Despite their similarities, the two lakes have some prominent differences that are summarized in Table S-1. In recent decades, Malo Jezero bottom waters have contained O_2 that fluctuated seasonally between about 50 and 150 μmol/L (Benović et al., 2000; Hrustić and Bobanović-Colić, 2017). However, Buljan and Špan (1976) reported that Malo Jezero's deep water column contained ΣS^{-II} concentrations in the 10–1000 μmol/L range during the 1950s. Strongly eutrophic Rogoznica Lake has generally higher chlorophyll and nutrient concentrations than Malo Jezero and is sulfidic at depth. Its sediments contain up to 6.7% organic carbon whereas Malo Jezero's sediments peak at 2.1%. Rogoznica's chemocline fluctuates in depth seasonally. In some years, it remains within 3 m of the sediment–water interface (Bura-Nakic et al., 2009a; Čanković et al., 2019). It is sometimes wiped out briefly in Autumn as oxic surface waters cool and mix downward before winter rains dilute them and restore water column stability. Past monitoring of ΣS^{-II} at 12 m shows that although Rogoznica's deep-water sulfide fluctuates, there has been a secular rise during recent decades (Čanković et al., 2019; Simonović et al., 2023).

2.2. Sampling

Water columns from both lakes were sampled using a clean Niskin water sampler. The samples were transferred from the Niskin water sampler to appropriate acid-cleaned perfluoralkoxy-polymer containers (Nalgene), transported to the laboratory, filtered under a nitrogen atmosphere, acidified with HNO_3 (69%, s.p., Rotipuran, Carl Roth, Karlsruhe, Germany) to a final concentration of 0.5% v/v, and stored at 5 °C. Water samples from Malo Jezero were syringe-filtered through 0.2-μm filters (cellulose acetate, Minisart, Sartorius), while those from the Rogoznica Lake were vacuum-filtered using 0.45-μm filters (cellulose acetate/nitrate, Millipore) due to very slow water drainage through 0.2-μm filters. Unacidified aliquots of water samples for the determination of sulfides from Rogoznica Lake were stored at 5 °C in clean glass bottles until analysis on the following day by voltammetry (Bura-Nakic et al., 2009a). Filters from Rogoznica Lake that contained visible amounts of suspended particulate matter (SPM) were freeze-dried under reduced pressure and stored for the determination of rhenium and trace elements in SPM.

Sediment samples from both lakes were collected using gravity corers. Cores were immediately capped and sealed, transported to the laboratory, and frozen at −20 °C until processing. Within two weeks after the collection, the sediments were thawed, sliced at 2-cm intervals under a nitrogen atmosphere, and transferred into appropriate plastic centrifuge vials. Porewater was separated from the sediment bulk by centrifugation at 4200 rpm for 15 min. Under a nitrogen atmosphere, porewater was decanted, filtered through 0.2-μm filters (Malo Jezero) or 0.45-μm filters (Rogoznica Lake), acidified with HNO_3 (s.p. grade) to a final concentration of 0.5% v/v, and stored by freezing at −20 °C. Unacidified aliquots of filtered porewater samples were frozen at −20 °C in 3-mL Eppendorf tubes for determination of sulfide.

Compacted sediment remaining after centrifugation was freeze-dried by lyophilization under reduced pressure, crushed, homogenized, pulverized, and stored at room temperature in sealed plastic zip-lock bags.

We collected one core from Rogoznica Lake in July and four cores from Malo Jezero, sampling this lake in April and November. On each visit to Malo Jezero, cores were taken at 24 m and 30 m water depth. Fig. S-1 in the Supplementary Material shows that appreciable variation in redox sensitive element concentrations were observed between the cores taken on the same date at two depths and between the cores taken at the same depth on different dates. In order to avoid an intricate discussion that would reveal little of general interest, we have opted in this paper to neglect these variations and to focus attention on the one Malo Jezero core with the highest redox sensitive element concentrations. However, the data for all cores are included in the Supplementary Material.

2.3. Sample preparation for rhenium and multielemental determinations

Rhenium in all sample types was determined using the isotope dilution (ID) approach. The amount of the ^{185}Re spike that was required to optimize quantification was estimated for every sample type by pre-analyzing several samples with external calibration.

For rhenium determinations in the Malo Jezero water column, 80–100 mL of seawater was spiked with enriched ^{185}Re standard tracer at least 24 h before extraction on ion-exchange columns. The samples were then acidified with HCl (35%, s.p., Rotipuran, Carl Roth, Karlsruhe, Germany) to a final concentration of 1 M. Due to expected low Re concentrations in Rogoznica Lake anoxic samples, samples were additionally preconcentrated by evaporation: 250–500 mL of aqueous sample was spiked with an appropriate amount of the ^{185}Re standard tracer, evaporated under sub-boiling conditions to approximately 30 mL, cooled down, filtered through a 0.2-μm filter, and acidified with HCl (s.p.) so that the final HCl concentration was 1 M.

For rhenium determination in porewaters, almost all of a sample (only 1 mL was retained for multielemental analysis) was spiked with the pre-estimated amount of enriched ^{185}Re standard tracer and acidified with HCl (s.p.) to a final concentration of 1 M at least 7 days before loading on the ion-exchange column. All water samples were loaded on the resin, as described below.

Soils and sediments for Re determinations were prepared using the following procedure. Between 50 and 80 mg of the sample was i) mixed with 5 mL HNO_3 (65%, p.a., Kemika, Zagreb, Croatia), 1 mL HCl (37%, VLSI Grade, Rotipuran, Carl Roth, Karlsruhe, Germany), 1 mL HF (47–51%, for trace analysis, Fluka, Buchs, Switzerland), ii) digested in a microwave oven, iii) mixed with 6 mL of 40 g/L H_3BO_3 solution (s.p., Fluka, Buchs, Switzerland) and iv) digested again in a Teflon bomb using a microwave oven (Multiwave 3000, Anton Paar, Graz, Austria) by ramping to 180 °C in 10 min and holding at 180 °C for 40 min. Limestone was digested in a similar manner but used HNO_3 s.p. and about 300 mg of sample. Digested samples were then quantitatively transferred to acid-cleaned PFA bottles, diluted with 25 mL of MQ, and stored until further processing (1 mL of this solution was retained for multielemental analysis). This solution contained high HNO_3 content and was unsuitable to be loaded on the ion-exchange column. Dellinger et al. (2020) and Faris and Buchanan (1964) showed that nitric acid does not interfere with Re adsorption on strongly basic ion-exchange resin if the HNO_3 concentration is <1 M. Therefore, the solution was transferred to an acid-cleaned Teflon container, spiked with the pre-estimated amount of enriched ^{185}Re standard tracer, and slowly evaporated (sub-boiling) to a volume of 0.5–1.0 mL, thus removing most of volatile acids (HCl and HF), while the remaining solution was probably a mixture of boric and nitric acid. The sample was then diluted with 25 mL of MQ water and acidified with HCl (s.p.) to the final HCl concentration of 1 M. Using this approach, the final content of HNO_3 in the solution was <0.6 M, which does not interfere with rhenium adsorption onto ion-exchange resin. Prepared samples were then loaded on the ion-exchange resin, as described below.

Filters with SPM were mixed with 4 mL of HNO_3 (s.p.) and digested in Teflon bombs using a microwave oven. Digested samples were then quantitatively transferred to acid-cleaned PFA bottles, diluted with 15 mL of MQ, and stored until further processing (1 mL of this solution was retained for multielement analysis). Further sample preparation is the same as described for sediment in the paragraph above. As the determination of Re in SPM was not initially planned, the mass of the empty filter was not measured and the estimated mass of SPM on filter is only approximate. Therefore, the results are provided in ng of Re per liter of filtered water.

2.4. Determination of rhenium

The rhenium ID spike was obtained from QMX Laboratories (UK) and the certified ^{187}Re/^{185}Re isotope ratio was 0.061. Rhenium in prepared samples was preconcentrated using an ion-exchange resin to remove isobaric interferences. The resin (Dowex 1X8, 100–200 mesh, chloride form) was first precleaned by soaking several times in 8 M HNO_3 (s.p.). Approximately 1 mL of the resin was transferred as a slurry in 8 M HNO_3 to a 4 mL polypropylene column (United Chemical Technologies) equipped with a porous frit (10 μm), rinsed with 5 mL of 8 M HNO_3 and cleaned with 5 mL of MQ water. The resin was finally preconditioned with 5 mL of 1 M HCl (s.p.). Rhenium was preconcentrated on the column by eluting a known volume of the sample (prepared as described above) through the column at a flow rate of approximately 0.5 mL min^{-1}. The preconcentrated Re was finally eluted from the column with 3 mL of 8 M HNO_3 (Bura-Nakić et al., 2021), as 6 portions of 0.5 mL.

Rhenium was determined using either high resolution-inductively coupled plasma-mass spectrometer (HR-ICP-MS; Element 2, Thermo Finnigan, Bremen, Germany) or inductively coupled plasma-triple quadrupole-mass spectrometer (ICP-QQQ-MS; Agilent 8800, Agilent, Santa Clara, USA), depending on the instrument availability. HR-ICP-MS was operated in hot plasma mode and ^{185}Re and ^{187}Re isotopes were measured at both low (LR) and medium (MR) resolution. For each sample, a total of 30 scans were performed (5 runs × 6 passes) to obtain good accuracy and precision. ICP-QQQ-MS was operated in hydrogen mode as preliminary tests demonstrated the absence of rhenium isotope fractionation. (The measured ^{187}Re/^{185}Re ratio in ID spike solution was 0.0611 ± 0.0028, n = 9, while in the Re standard solution (ASTASOL® AN90461H) the ratio was 1.6730 ± 0.0154, n = 13, which is similar to the natural abundance ^{187}Re/^{185}Re ratio of 1.6738). For each sample, a total of 300 scans were performed (30 runs × 10 passes) to obtain better accuracy and precision, as the ICP-QQQ-MS is not a high-resolution instrument.

Several blank samples, certified reference materials (CASS-4, MESS-3, NCS DC 75301), duplicate parallel samples, and samples spiked with natural abundance Re were always prepared to assess the detection limit, accuracy, reproducibility, and recovery of the analytical procedure for both water and sediment samples. The amount of rhenium in samples was always corrected for rhenium in the corresponding blank sample. Comparison of measured Re content in certified reference materials with the literature values is presented in section B of the Supplementary Materials. The method reproducibility was assessed by duplicate parallel samples prepared following the whole analytical procedure (including sample digestion for sediments) whose difference was always lower than 6%, thus confirming good sample homogeneity and analytical performance. The average recoveries of natural abundance Re spikes from water and sediment samples were 97.2% and 100%, respectively, indicating that both ^{185}Re enriched spike and isotopically normal Re show similar behavior in the sample matrix and on the ion-exchange resin.

2.5. Multielemental determinations

Depending on the instrument availability, HR-ICP-MS or ICP-QQQ-MS were used for the determination of elemental concentrations in water, soil, sediment, and SPM samples. The water samples for the analyses were prepared in pre-cleaned polyethylene tubes by 10-fold

dilution of seawater/porewater in 2–5% HNO_3 (s.p.) and using ^{115}In or ^{103}Rh as an internal standard. The calibration was performed using an external calibration in seawater. For soil and sediment samples, we applied a 100-fold dilution of digested samples in 5% HNO_3 (s.p.) and used ^{103}Rh as an internal standard. The calibration was performed using an external calibration in 5% HNO_3 (s.p.).

Quality control of HR-ICP-MS and ICP-QQQ-MS measurements in water was checked by analyzing certified standard reference materials (CASS-4 and CASS-5, National Research Council Canada, Ontario, Canada). For soils and sediments, certified reference material NCS DC 75301 (China National Analysis Centre for Iron and Steel, Beijing, China) was used. A good agreement with the certified data was obtained for all investigated elements and matrix (see Section B, Supplementary Material). Limits of detection (LODs) were calculated as three times the standard deviation of procedural blanks (including digestion). The typical LODs for Mo, Re, U, and Al in sediments were 25 ng/g, 0.08 ng/g, 0.5 ng/g, and 7 μg/g, respectively. The LODs for Mo, Re, and U in water samples were 0.1 μg/L, 0.05 ng/L, and 0.01 μg/L, respectively.

2.6. Modeling Mo and Re solubility

To interpret Re_{aq} and Mo_{aq} profiles in Rogoznica's euxinic waters, we employ a model that attributes Mo_{aq} and Re_{aq} scavenging to their mutual coprecipitation in $Fe(Mo,Re)S_4$ nanoparticles as described by Vorlicek et al. (2018), Helz and Vorlicek (2019) and Helz (2022). The model requires data for only ΣS^{-II} and pH. We found that we could fit measured pH values *versus* depth in Rogoznica Lake by linear segments in the sulfidic waters and could fit ΣS^{-II} by a quadratic equation (see Fig. S-6, Supplementary Material). We used these functions for smoothing and interpolating between sampling horizons in the water column. The solubility of the coprecipitate phase is assumed to be the same as endmember $FeMoS_4$ (Vorlicek et al., 2018), because the mole fraction of Re in Mo sites will always be $<10^{-3}$. We set Q_{FeS} to $10^{-4.87}$, the value appropriate for FeS nanoparticles. The model yields concentrations of total dissolved Mo, which includes not only MoO_4^{2-} and the thiomolybdates, but also the Fe-Mo-S complexes characterized by Helz et al. (2014).

Where we discuss concentrations of authigenic components in solid phase materials, a correction for a lithogenic contribution will have been made using a conventional formula:

$$E_{auth} = E_{obs} - Al_{obs}\left(\frac{E}{Al}\right)_{litho} \quad (1)$$

where E represents Mo, Re or U, and $[E/Al]_{litho}$ is the ratio of the element to Al in a representative lithogenic material. E_{auth} values are not very sensitive to the choice of lithogenic reference material because suspended particles and sediments in the two lakes are highly enriched relative to lithogenic materials and Al_{obs} tends to be small in the carbonate-dominated sediments. Generally, E_{auth} is >99% of E_{obs}.

Where we discuss Re/Mo mass ratios in either the aqueous or solid phase, we will normalize them to seawaters' dissolved ratio of 0.000735; normalized ratios will be designated by a subscript *sw*. Normalization is a convenient way to suppress superfluous zeros in the data and to facilitate comparison of the composition of seawater to the composition of its sedimentary products.

Where we discuss Rayleigh fractionation of Re_{aq} with respect to Mo_{aq} during coprecipitation, the concentration of Re_{aq} will be calculated from:

$$Re_{aq} = Mo_{aq}\left(\frac{Re_{aq}}{Mo_{aq}}\right)^0 f^{\alpha-1} \quad (2)$$

where $[Re_{aq}/Mo_{aq}]^0$ is the ratio of the dissolved concentrations of the two elements before any coprecipitation has occurred, f is the fraction of Mo_{aq} remaining in solution after some amount of coprecipitation has occurred and $\alpha = [Re_s/Mo_s]/[Re_{aq}/Mo_{aq}]$ = the partition coefficient. Finally, where we discuss the composition of cumulative $Fe(Mo,Re)S_4$ coprecipitates, the product's composition will be calculated from:

$$\left(\frac{Re_{auth}}{Mo_{auth}}\right)_{sw,cum} = \left(\frac{Re_{aq}}{Mo_{aq}}\right)^0_{sw}\left(\frac{1-f^{\alpha}}{1-f}\right), \quad (3)$$

3. Results

3.1. General redox characteristics

Fig. 1 shows redox indicator properties in the water columns and pore waters of the two lakes. In Malo Jezero, the water column is oxic down to the sediment–water interface. When our samples were collected, water column salinity ranged from 36 at the top to 39 at the bottom. Step increases by >100-fold in Mn_{aq} and Fe_{aq} concentrations and the first appearance of ΣS^{-II} occur in shallow pore waters; pore water pH shifts downward from 8.3 at the interface to an average of 7.5 below −0.1 m depth in sediments, and total sulfide (ΣS^{-II}) rises to only about 25 μmol/L.

In Rogoznica Lake, a chemocline existed between 7 and 9 m above the sediment–water interface when our samples were taken in July 2021. Salinity in the water column spanned a small range from 34 at the top of the water column to 36 at the bottom. In the downward direction across the chemocline, Mn_{aq} jumps by 10-fold, Fe_{aq} by 16-fold and ΣS^{-II} by 3000-fold, the latter reaching values exceeding 2000 μmol/L. Production of H^+, mainly by biological sulfate reduction, drives pH down across the chemocline from 8.2 to 7.2, and drives it further to below 6.8 in pore waters (see data tables in Supplementary Material).

In both lakes, the O_2-ΣS^{-II} transition in the downward direction is marked by a large release of Mn_{aq} (Fig. 1). In Rogoznica, where this transition is observable in the water column, a corresponding large decrease of Mn_s in suspended particles occurs (Fig. 2A). At greater depths, Mn_s in suspended particles as well as Mn_{aq} change little, although Mn_{aq} in the sediments of both lakes undergoes a gradual downward decline that could be related to a corresponding slight increase in pH (Fig. 1), which lowers the solubility of Mn carbonates. A thermodynamic speciation calculation employing published DIC measurements (Pjevac et al., 2019) suggests that beneath the O_2-ΣS^{-II} transition, Mn_{aq} is controlled by saturation with $CaMn[CO_3]_2$ (pseudokutnahorite; thermodynamic data of Mucci, 2004). At the chemocline, Mn(III,IV) oxyhydroxides are presumed to be transformed to $CaMn[CO_3]_2$ and do not reach sediments except when mixing events oxygenate the entire water column..

Contrary to the Mn_s pattern, concentrations of Fe_s in suspended particles in Rogoznica's water column sharply rise in the chemocline region before gradually declining past a peak near 7 m (Fig. 2A). The righthand panel shows that downward through the chemocline the Q_{FeS} activity product ($=[Fe^{2+}][H_2S]/[H^+]^2$) in bulk water rises steeply until becoming fixed in a range characteristic of equilibrium with FeS precipitates. The Q_{FeS} values imply saturation with respect to FeS phases having solubilities intermediate between those of crystalline mackinawite and amorphous FeS. These Q_{FeS} values characterize bulk water; higher values are expected in microbial hotspots (microniches), where supersaturation must occur before FeS nanoparticles can nucleate.

However, if the authigenic iron precipitates appearing near Rogoznica's chemocline were exclusively FeS (with or without some authigenic pyrite), it would be puzzling why particulate Fe_s declines downward through the sulfidic water column (Fig. 2A), given that the solution remains saturated with FeS phases (Fig. 2B) and that pyrite precipitation is irreversible under reducing conditions. Very likely, authigenic Fe(III) oxyhydroxides also form near the chemocline owing to mixing of Fe^{2+} from deeper waters with O_2 from shallower waters. As Fe(III)-bearing particles settle into the sulfidic zone, some will react with sulfide and gradually dissolve, thus explaining the loss of particulate Fe_s below 7 m. Apparently, though, not all particulate Fe(III) is consumed within the water column of this shallow lake. The large ΣS^{-II} deficit

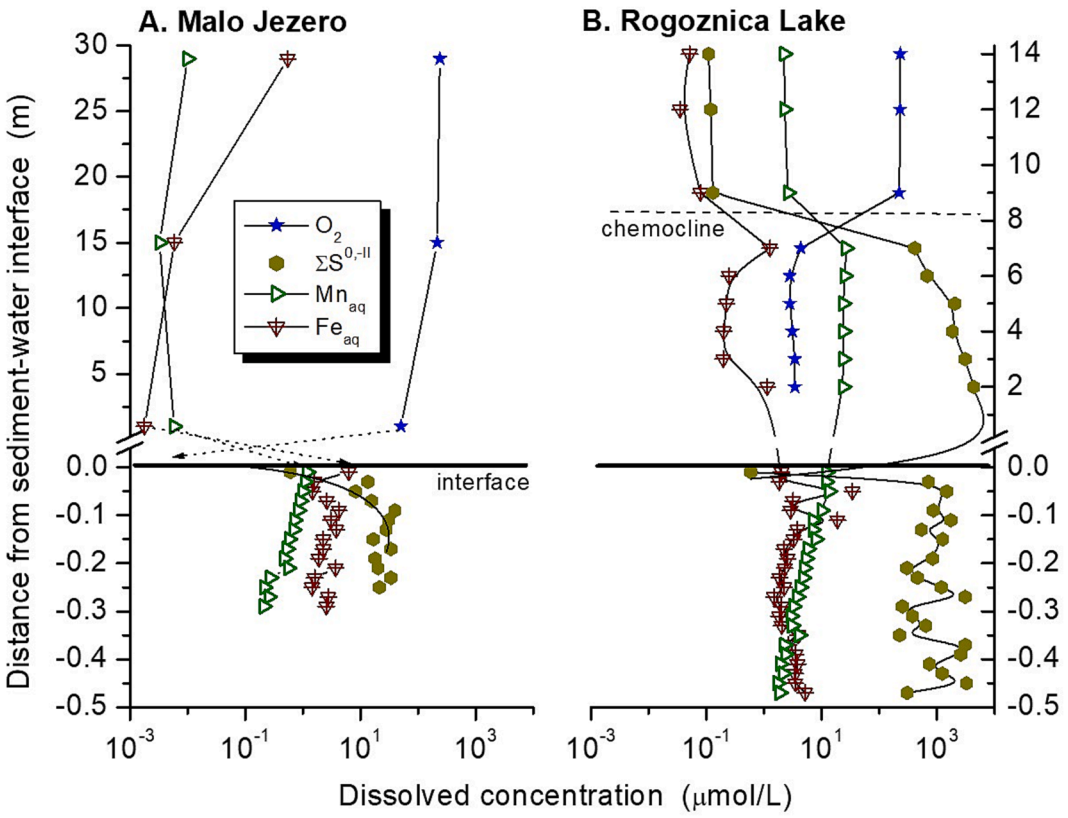

Fig. 1. Water column and pore water composition of Malo Jezero and Rogoznica Lake. These Malo Jezero data were obtained in November 2021 and the Rogoznica Lake data in July 2021. $\Sigma S^{0,-II}$ is the sum of zero-valent and divalent sulfur as determined by voltammetry; above the chemocline, zero-valent sulfur predominates and below, divalent sulfide predominates (Bura-Nakic et al., 2009a). Note scale breaks on the vertical axes.

shown in Fig. 1 at the sediment–water interface in Rogoznica Lake implies that significant amounts of oxidative particles survive to accumulate and react with sulfide at the sediment–water interface. Fig. 1 shows that in the −0.01 to −0.02 m depth interval in Rogoznica's pore waters, ΣS^{-II} equals a scant 0.6 μmol/L (below the detection of some analytical methods). This is much lower than in samples immediately above and below it. Maintenance of this deep sulfide well at the interface requires a steady supply of reactive, oxidizing particles. Particulate Fe_s averages 4.7 mg/g at 0.00 to −0.05 m of sediment and 2.7 mg/g below −0.10 m, confirming loss of Fe_s during burial.

3.2. Redox-sensitive trace elements

Figs. 3 and 4 show sediment and water column data for Malo Jezero and Rogoznica Lake respectively. A first impression of these data is that the patterns for all three redox sensitive elements are quite similar. Mutual correlations between the three elements in sediments are positive and highly significant (all $p < 0.0001$) in both lakes (Fig. S-2).

Figs. S-3–S-5 in the Supplementary Material present correlations between these three elements and Al (a lithogenic proxy), Sr (a carbonate proxy, especially for aragonite) and Ba (a biological productivity proxy). Those correlations are mostly of low significance ($p > 0.01$) and negative. Exceptions are significant positive correlations of all three redox sensitive elements with Al in Malo Jezero. Negative correlations imply that the components that those proxy elements stand for are more likely to be diluents than sources of the redox sensitive elements.

In Malo Jezero, the range of salinity-normalized concentrations for Mo_{aq}, Re_{aq} and U_{aq} in the water column are respectively 95–110 nM, 34–40 pM and 11–13 nM, which are similar to seawater concentrations. The results are consistent with overall experience that these elements exhibit little reactivity in oxic waters. Chemical processes that measurably affect redox sensitive element concentrations are confined to sediments in this lake.

In contrast, in Rogoznica Lake scavenging depletes seawater normalized Re_{aq} in the oxic zone by about 50% and U_{aq} by about 30% while having a negligible effect on Mo_{aq} (Fig. 4). These elements' aqueous concentrations are constant vertically in the oxic zone, indicating that scavenging is slow in relation to vertical mixing within this zone, but particulate $[E/Al]_s$ ratios (E = Mo, Re or U) rise downward, indicating that all three elements experience some scavenging. In eleven previously published Mo_{aq} profiles obtained at various times of year (Helz et al., 2011a; Bura-Nakić et al., 2018), salinity-normalized Mo_{aq} in Rogoznica's oxic water usually corresponds closely to its value in seawater. Exceptions occur during episodic deposition of North African dust, when surface waters become greatly enriched in Mo_{aq}. Salinity-normalized U_{aq} in oxic Rogoznica water is consistently depleted relative to seawater in the larger dataset, even during dust deposition episodes (Bura-Nakić et al., 2018). No previous data for Re_{aq} are available.

In Rogoznica Lake, the lowest E_{aq} concentrations and highest $[E/Al]_s$ ratios for all three elements are found in the middle, sulfidic zone of the water column. $[Re/Al]_s$ and $[Mo/Al]_s$ ratios reach plateaus a short distance beneath the chemocline, implying that net scavenging of these elements from the deeper sulfidic zone is negligible despite rising ΣS^{-II}. As discussed later, when plotted on a linear, rather than logarithmic scale, the $[U/Al]_s$ profile is seen to be subtly different.

In Table 1, the $[E/Al]_s$ (E = Mo, Re or U) ratios in sediments are compared to upper continental crust (UCC), and local Terra Rossa soils. Included in the table are several of Bennett and Canfield's (2020) enrichment thresholds proposed to aid in classifying the redox status of depositional environments. The thresholds misclassify the Croatian lakes' sediments. For example, $[E/Al]_s$ ratios in the shallowest Malo Jezero sediments (line 6 in the table), which were deposited under modern oxic conditions, are most similar to Bennett and Canfield's euxinic thresholds (line 7) and contain far more Mo, Re and U relative to

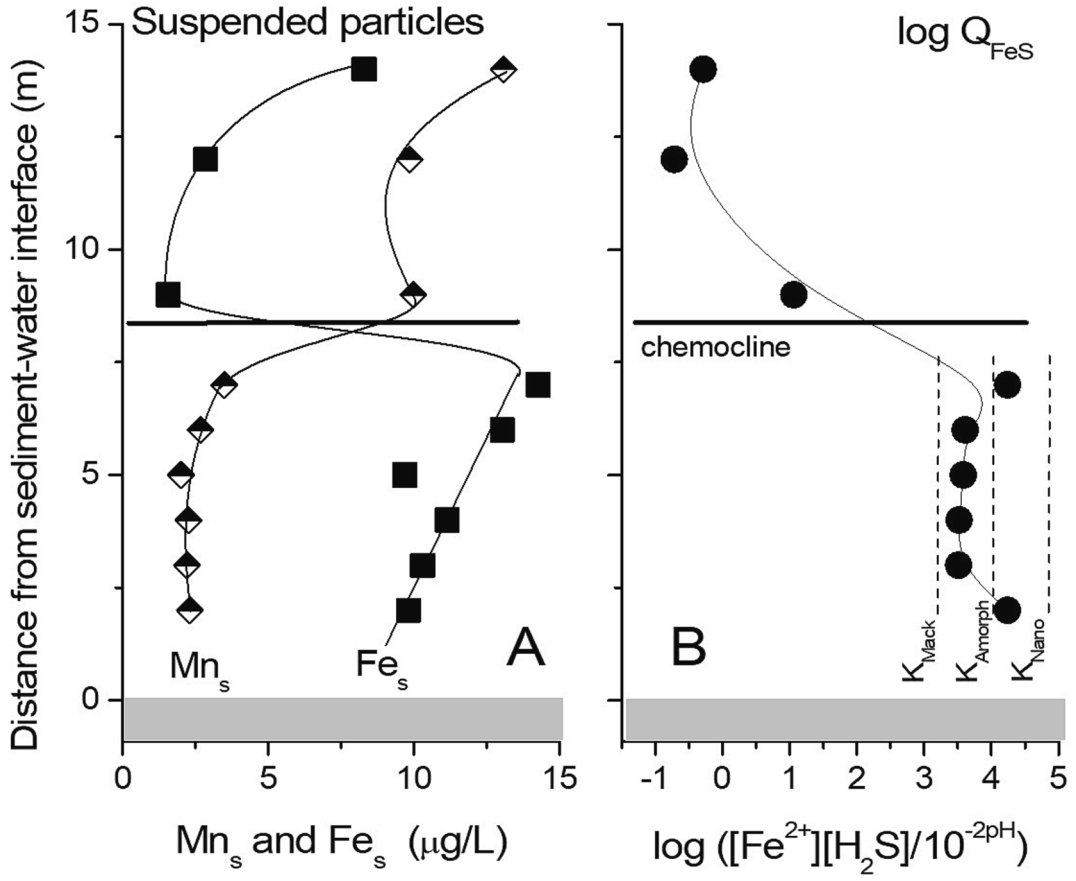

Fig. 2. A: Fe_s and Mn_s in suspended particles in Rogoznica's water column. B: Comparison of solubility constants for mackinawite, amorphous FeS and nano FeS to the FeS ion activity product profile in the water column. The calculated $[Fe^{2+}]$ activity included corrections for complexing by Cl^-, SO_4^{2-}, CO_3^{2-}, HS^- and MoS_4^{2-}. Solubility constants from Davison (1991), Benning et al. (2000) and Wolthers et al. (2005).

Al than oxic basin sediments (line 11). This result is due to low Al in the carbonate-rich sediments of the Croatian lakes.

Taking UCC as the reference material for calculating enrichment factors, Rogoznica's are 830, 300 and 30 for Mo, Re and U respectively. These values approach those in so-called highly enriched black shales. Malo Jezero's enrichment factors are less striking but nonetheless quite large: 170, 180, and 7.9. If local Terra Rossa soils (residues of limestone weathering modified by aeolian dust from North Africa) are chosen as the reference material, enrichment factors are substantially lower but still large: Rogoznica's are 170, 15, and 23 for Mo, Re and U respectively and Malo Jezero's are 35, 8.7 and 6.2.

Curiously, Rogoznica's water column suspended particles (line 4, Table 1) have much higher $[Re/Al]_s$ and $[Mo/Al]_s$ ratios than particles accumulating in underlying sediments (line 2; also see Fig. 4). In part, this can be attributed to seasonal effects. Suspended particle concentrations record transitory conditions whereas sedimented particle concentrations record time-composites. Our Rogoznica Lake suspended particles were collected in July, which is a season of high photosynthetic C_{org} production, which drives high sulfide production in the deep waters (Bura-Nakic et al., 2009a). Introduction of aluminous particles by erosion of the watershed and by rainout/washout of aeolian dust are near annual minima during this dry period (Mifka et al., 2022). This combination of conditions favors high $[Re/Al]_s$ and $[Mo/Al]_s$ on suspended particles in summer. Long-term averages registered by sediments will be lower because of higher Al input in the wet season. In contrast, $[U/Al]_s$ is less affected by seasonal variations (Table 1), because it is not directly affected by sulfidic conditions in the water column, as discussed later.

Our measured Mo_{aq} and U_{aq} concentrations in Rogoznica's pore waters exceed those reported by Bura-Nakić et al. (2018) by ≈50-fold. As discussed later, this disparity probably arises from differences in methodology. Our pore water concentrations were determined after centrifuging sediment samples under anaerobic conditions and then taking up the solution by syringe through 0.45 μm filters. After similarly centrifuging, Bura-Nakić et al. (2018) took up the solution through Rhizon samplers (0.15 μm pore size).

4. Discussion

Understanding how Life originated and evolved is one of the big problems challenging 21st century science. Life's evolution is documented by fossils only over the last tenth of Earth's history. Before that, in the Precambrian, the fossil record fades out both because older rocks have suffered more damage by geologic processes and because very few earlier organisms produced recognizable, geologically resilient structures. Therefore, the record of Life's evolution during the Precambrian is reconstructed largely from proxies—molecular, elemental or isotopic signatures that in sedimentary basins are controlled directly or indirectly by biological processes. The signatures' behaviors in modern environments are most often the basis for inferences about Life in ancient environments. An always precarious assumption is that Life's evolution has not changed this behavior over time in unknown ways. Understanding any proxy's mechanism at a fundamental chemical or biochemical level can enhance confidence in this assumption.

In the following sections, we test how well $[Re_{auth}/Mo_{auth}]_{sw}$ ratios calculated from our data serve as a proxy for the known redox history of the two Croatian lakes, and how well the chemical mechanism proposed by Helz (2022) can explain the data. Consistent with previous work, we

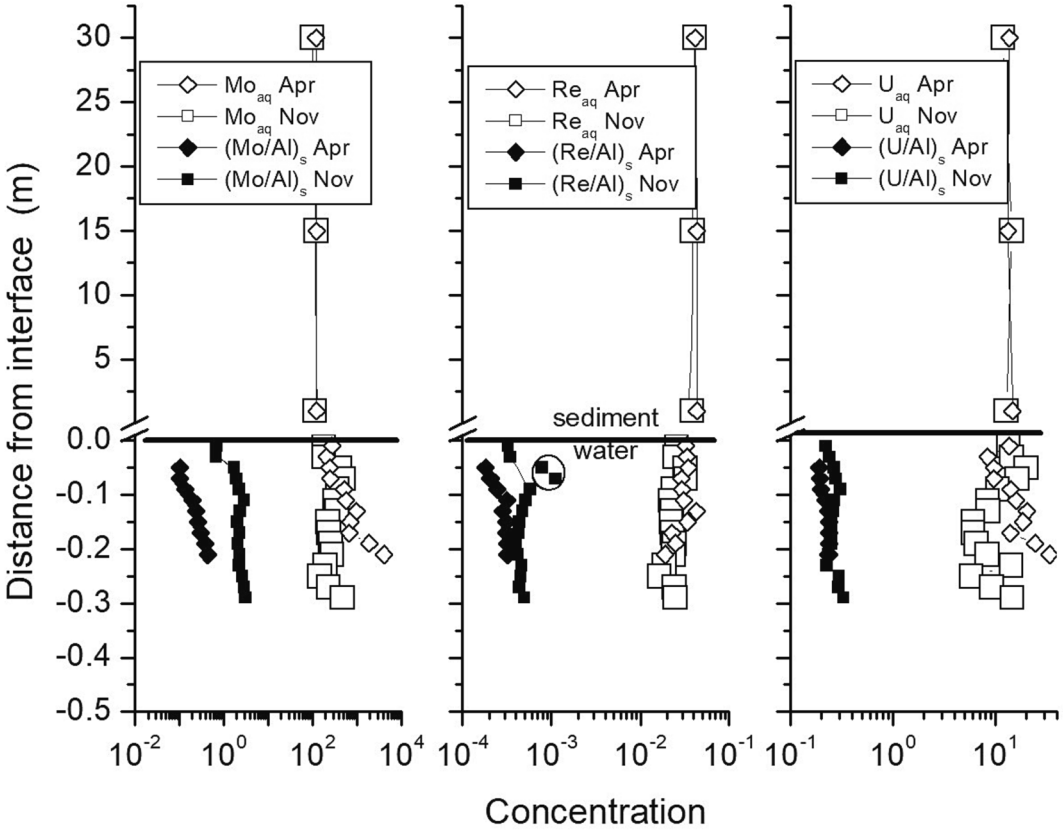

Fig. 3. Overview comparing Mo, Re and U distributions in Malo Jezero cores taken at 30 m water depth in April and November 2021. Aqueous concentrations in nmol/L for Mo, Re and U and these elements' solid phase ratios to Al in mg/g. Data for particulate material in the water column could not be obtained because of paucity of material in these oligotrophic to mesotrophic waters. In the middle panel, two $[Re/Al]_s$ outliers (circled) occurred at 5 and 7 cm depth. Note vertical scale break at the sediment–water interface.

will also show that U is controlled by a different mechanism than Mo and Re despite the high degree of correlation ($p < 0.0001$) between all three elements in both lakes (shown in Fig. S-2).

4.1. $[Re_{auth}/Mo_{auth}]_{sw}$ fractionation

Fig. 5A tracks the seawater-normalized authigenic rhenium/molybdenum ratios in the sediments of the two lakes. For Rogoznica Lake sediments, which underly a water column that is normally sulfidic but in some years becomes hypoxic after overturn in Autumn (see data in Barić et al., 2003; Dominovic et al., 2023), $[Re_{auth}/Mo_{auth}]_{sw}$ values are similar to those in basins like the Saanich Inlet and the Gotland Deep, which are mostly euxinic but experience oxygenation at irregular intervals (refer to Figure 2 and references in Helz, 2022). A gradual decline in Rogoznica's $[Re_{auth}/Mo_{auth}]_{sw}$ in the upward direction may be indicative of the known secular trend toward more sulfidic conditions during the last several decades, as described by Čanković et al. (2019) and Simonović et al. (2023).

Fig. 5A shows that the trend in Malo Jezero is in the opposite direction. This is consistent with old reports that during the 1950s Malo Jezero's water column was sulfidic, like Rogoznica's today, but has gradually become oxic (discussed by Bura-Nakić et al., 2020). Sondi and Juračić (2010) estimate that Malo Jezero's sedimentation rate is ≈0.26 cm/yr. If this rate is valid for our core, then 1950s sediment would be found today at −0.15 to −0.18 m depth. Compared to the core obtained from 30 m water depth, the 24 m Malo Jezero core has progressed further in the shift to higher $[Re_{auth}/Mo_{auth}]_{sw}$, suggesting that it has experienced more extensively oxic conditions. Dissolved oxygen profiles published by Benović et al. (2000) and Hrustić and Bobanović-Colić (2017) show that this is likely to have been true. The evolution of $[Re_{auth}/Mo_{auth}]_{sw}$ in Malo Jezero is consistent with the findings of Bennett and Canfield (2020) that sediments deposited under oxic waters are commonly Re-enriched compared to upper continental crust (line 11, Table 1).

An alternate interpretation of Malo Jezero's $[Re_{auth}/Mo_{auth}]_{sw}$ trend might invoke a hypothetical diagenetic process that either releases Re_s or fixes Mo_s as sediments become buried. Such a process ought to reveal itself in pore waters' dissolved Re_{aq} or Mo_{aq} profiles. Fig. 3 discloses no evidence of Re_{aq} or Mo_{aq} trends that would support this hypothesis. Data in the Supplementary Material show that Mo_{aq} increases, rather than decreases, while Re_{aq} changes very little with increasing depth in all four Malo Jezero cores that we studied.

For comparison, Fig. 5B and C reproduce the $\delta^{98}Mo_{auth}$ and $\delta^{238}U_{auth}$ data presented and discussed by Bura-Nakić et al. (2018, 2020). While these data can be rationalized based on the known historical evolution of redox conditions in these lakes, the data do not produce the compelling record of change presented by the $[Mo_{auth}/Re_{auth}]_{sw}$ record.

4.2. Aqueous phase evidence of Re and Mo coprecipitation

As shown in Fig. 5A, all Rogoznica sediment samples as well as most of the deepest Malo Jezero samples have $[Re_{auth}/Mo_{auth}]_{sw}$ ratios that are substantially lower than lithogenic source materials such as Terra Rossa soils and upper continental crust (see also Table 1). Thus, they cannot be simple mixtures of material from these sources. The ratios are also lower than typical euxinic and oxic basin sediments, as these have been characterized by Bennett and Canfield (2020; line 11, Table 1). Now we will show that $[Re_{auth}/Mo_{auth}]_{sw}$ ratios in Rogoznica's water and suspended particles, *but not its sediments*, can be explained reasonably well solely by coprecipitation of Re and Mo in $Fe(Mo,Re)S_4$ in the

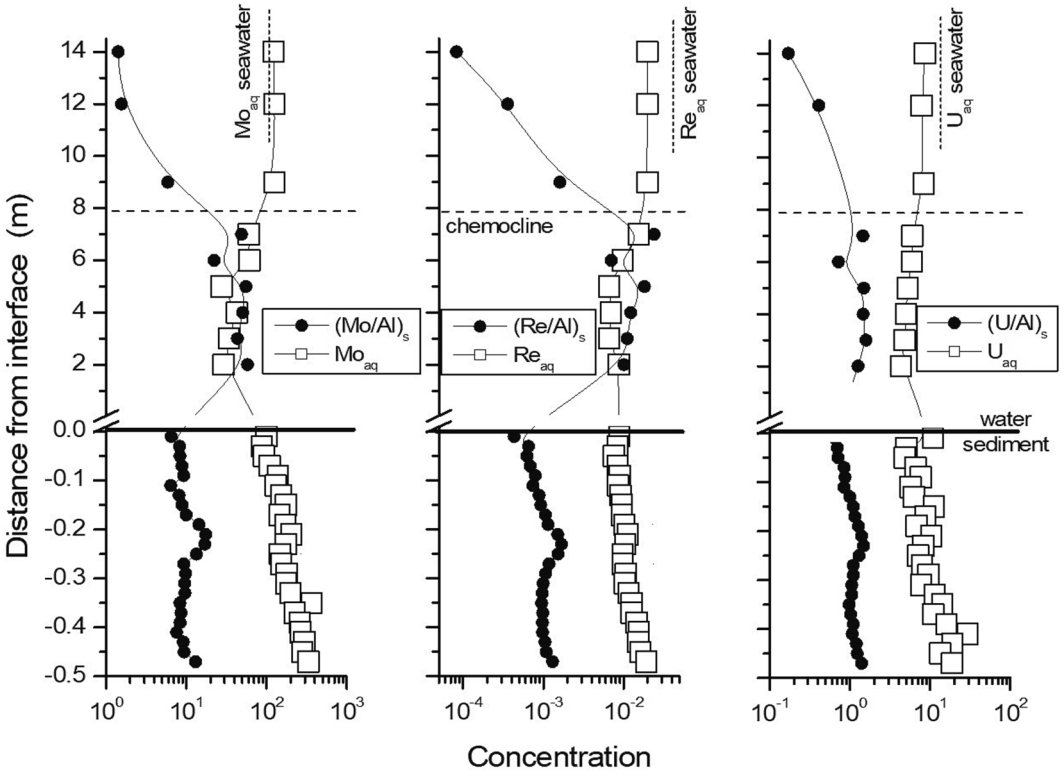

Fig. 4. Overview comparing Mo, Re and U distributions in Rogoznica Lake in July 2021. Aqueous concentrations given in nmol/L and solid phase $[E/Al]_s$ ratios in mg/g. Seawater aqueous concentrations of the elements are marked by vertical dotted lines for reference. The E_s peak for all three elements near −0.2 m in the sediments is caused by simultaneous positive excursions in the trace element concentrations, not a negative excursion in Al_s concentrations. Other elements showing a pronounced peak at this depth are Mn_s, Co_s and Ni_s (unpublished data). These, along with Mo_s and to a lesser extent U_s, are commonly enriched in marine ferromanganese deposits (Hein et al., 2013).

Table 1
Average unitless mass ratios in selected materials ordered by $[Re/Mo]_{sw}$.

	$[Mo/Al]_s$	$[Re/Al]_s$	$[U/Al]_s$	$[Re/Mo]_{sw}$*
1. Marine Fe,Mn crusts and nodules (JMn-1)†	1.4×10^{-1}	2.2×10^{-9}	2.2×10^{-3}	0.00021
2. Rogoznica Lake sediments (n = 24)	1.0×10^{-2}	1.0×10^{-6}	1.3×10^{-3}	0.16
3. Malo Jezero sediments (Nov, depth −0.1 to −0.29 m)	2.5×10^{-3}	4.6×10^{-7}	2.7×10^{-4}	0.25
4. Rogoznica Lake sulfidic water suspended particles	4.6×10^{-2}	1.2×10^{-5}	1.3×10^{-3}	0.36
5. Upper continental crust (Chen et al., 2016)	1.1×10^{-5}	3.1×10^{-9}	3.3×10^{-5}	0.37
6. Malo Jezero sediments (30 m Nov, depth 0 to −0.05 m)	1.0×10^{-3}	4.9×10^{-7}	2.4×10^{-4}	0.67
7. Euxinic basin sediments (Bennett and Canfield, 2020)	1.3×10^{-3}	1.0×10^{-6}	3.8×10^{-4}	1.0
8. Terra Rossa soils (n = 4, this work & Sondi et al., 2017)	5.5×10^{-5}	6.3×10^{-8}	4.2×10^{-5}	1.7
9. Seasonal OMZ sediments (Bennett and Canfield, 2020)	2.1×10^{-4}	2.9×10^{-7}	6.7×10^{-5}	1.9
10. Malo Jezero sediments (24 m Nov, depth 0 to −0.05 m)	1.8×10^{-4}	3.5×10^{-7}	2.6×10^{-4}	2.6
11. Oxic basin sediments (Bennett and Canfield, 2020)	1.6×10^{-5}	6.5×10^{-8}	3.1×10^{-5}	5.5

* Normalized to Re/Mo ratio in modern seawater (mass ratio = 0.000735).
† Ferromanganese nodule standard: Imai et al., 1999; Tagami and Uchida (2007).

water column.

Concentrations of Re_{aq} and Mo_{aq} have been plotted together in Fig. 6 on a linear scale. Below the chemocline, both Mo_{aq} and Re_{aq} drop quickly to asymptote concentrations that are poised distinctly above analytical detection limits. It is noteworthy that Re_{aq} seems to begin declining in the sulfidic water column just where Mo_{aq} does, and arrives at its asymptote at 5.5 m depth, just where Mo_{aq} does. Though our vertical resolution is admittedly poor, these aqueous phase data lend no support to the view of Crusius et al. (1996) that Re_{aq} is removed before Mo_{aq}. For Re_{aq}, the asymptote values are maintained down through shallow pore waters. In deeper pore waters, Re_{aq} rises gradually, reaching about 19 pmol/L at the core bottom. Asymptote patterns for Re_{aq} have been recognized elsewhere by Morford et al. (2012), who cite more than a dozen examples of Re_{aq} asymptotes that fall in the 3.8——16 pmol/L range. For Mo_{aq}, the asymptote value is 25 nmol/L in the water column but is not observed in pore waters in our dataset.

Curves from the coprecipitation model are compared to the data in Fig. 6. The model assumes that downward in the water column, as ΣS^{-II} rises and pH declines, $Fe(Mo,Re)S_4$ begins to precipitate irreversibly where its solubility falls below ambient Mo_{aq} and continues to do so until its solubility minimum is reached (Helz, 2022). In July in Rogoznica Lake, the solubility minimum calculated from smoothed and interpolated values of ΣS^{-II} and pH (see Fig. S-6, Supplementary Material), occurred at 5 to 6 m above the sediment–water interface. Below that depth, the dashed curve in Fig. 6 traces the rise in solubility calculated from the further increases in ΣS^{-II} and declines in pH. For the Mo concentration in the water to follow the dashed curve below the solubility minimum, new Mo_{aq} must be supplied to the aqueous phase from particles. The new Mo_{aq} cannot come from dissolving $Fe(Mo,Re)S_4$ precipitates. Once $Fe(Mo,Re)S_4$ forms, it undergoes an irreversible transformation that prevents its redissolution in the absence of oxidizing agents (demonstrated by Vorlicek et al., 2018). The solid curve traces the expected Mo_{aq} asymptote profile if no sufficiently reactive particulate material is available to resupply Mo_{aq}. The figure shows that the observations are best described by the solid curve.

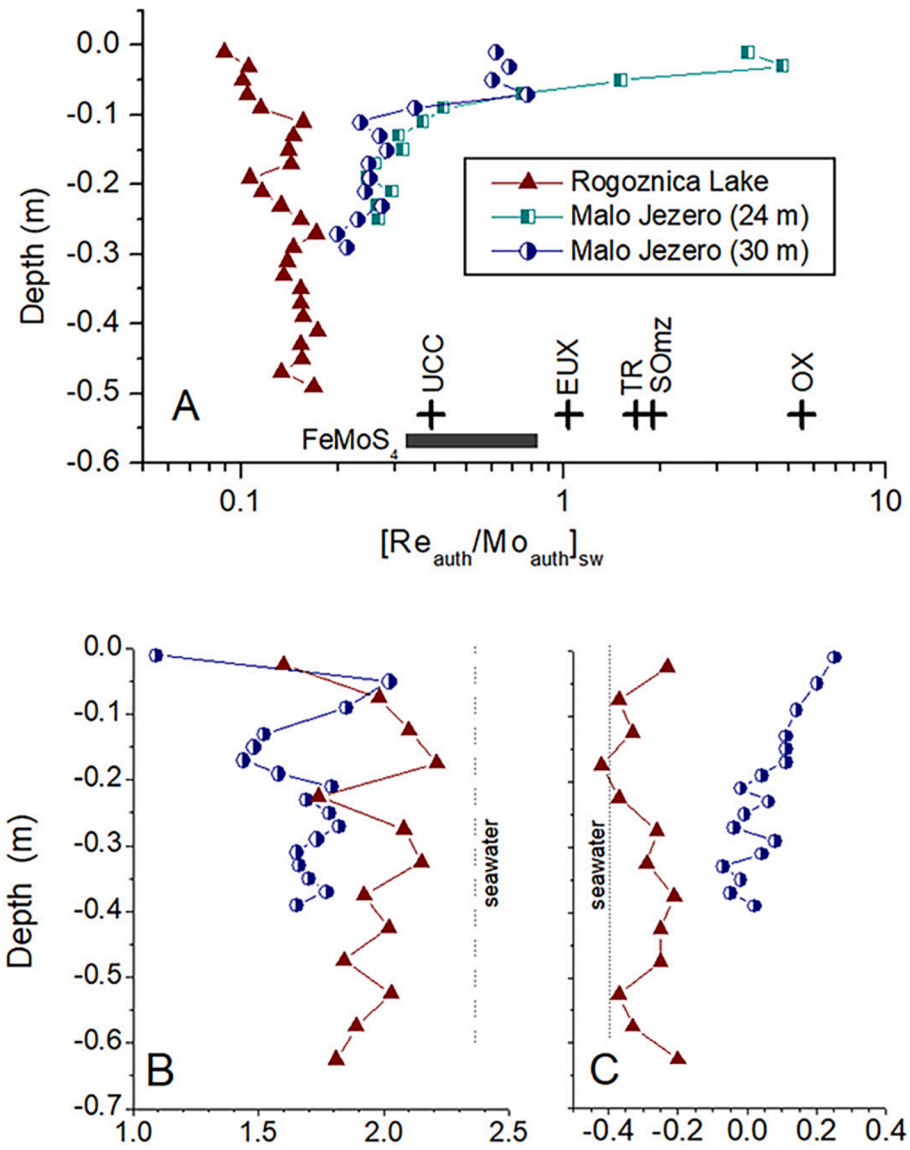

Fig. 5. A. Authigenic Re/Mo ratio in the sediments of Rogoznica Lake (July 2021 core) and Malo Jezero (November 2021 cores). Analytical uncertainty in the ratios is similar to the size of the symbols. Plotted near the bottom of Panel A are reference ratios from Table 1: UCC-upper continental crust, EUX-euxinic sediments, TR-Terra Rossa soils, SOmz-seasonal oxygen minimum zone sediments and Ox-oxic sediments. The bar showing the modelled composition range of $FeMoS_4$ precipitates is discussed in the text. B. and C. Respectively, $\delta^{98}Mo$ and $\delta^{238}U$ data from Bura-Nakić et al. (2018, 2020).

Notice that under the highly sulfidic conditions prevailing a few meters above the sediment–water interface in Fig. 6, Mo_{aq} potentially can reach concentrations several times larger than in seawater before becoming limited by $Fe(Mo,Re)S_4$ saturation, which is indicated by the green dashed curve. Contributing to this high calculated solubility are Fe-Mo-S complexes, including $[(Fe_2S_2)(MoS_4)_2]^{4-}$ dimers. Table 2 shows the calculated distribution of the most important dissolved Mo species. The table shows, for example, that at two meters above the sediment–water interface, calculated Mo_{aq} at saturation is 225 nM (twice seawater); 93% consists of $[(Fe_2S_2)(MoS_4)_2]^{4-}$ dimers. That dimers can become stable at $Mo_{aq} < 10^{-7}$ M in highly sulfidic, mildly acidic waters is noteworthy because the chemical conditions that promote monomer → dimer transitions are apt, when pushed farther, to promote polymerization, producing ferrothiomolybdate colloids (see below).

The high Mo_{aq} concentrations predicted at saturation with $Fe(Mo,Re)S_4$ (dashed green curve, Fig. 6) are not observed in Rogoznica's deepest water column. Iron(III) oxyhydroxide particles that could release Mo_{aq} by reductive dissolution apparently are insufficiently reactive to affect the Mo_{aq} composition of the lower water column as they pass through it.

Experimental studies show that reduction rates of Fe(III) phases are variable and can be divided into two groups (Poulton et al., 2004). Ferrihydrite and lepidocrocite are fast reacting. These phases might be produced rapidly in the vicinity of the chemocline if Fe^{2+} and O_2 come into contact. Probably, they would be substantially consumed by reaction with sulfide as they settled toward the sediment, explaining the observed decline in particulate Fe_s shown in Fig. 2. Goethite, hematite, magnetite and Fe-bearing silicates are slow reacting. Goethite and hematite are the characteristic minerals of the Terra Rossa soils in the surrounding watersheds and are known to be important Mo hosts in karst terrane soils (Lin et al., 2023). These slow reacting phases apparently settle through the 7 m water anoxic column too quickly to react appreciably with sulfide until after they reach the sediment–water interface. The importance of these phases lies in their ability to capture substantial amounts of Mo and U (Hein et al., 2013), while rejecting Re (Koide et al., 1986; McDaniel et al., 2004; Tagami and Uchida, 2007). Even over a broad pH range, hematite and powdered marine ferromanganese material sorb negligible ReO_4^- (Yamashita et al., 2007). Fig. 6 shows that high Mo_{aq} does appear in the pore waters beginning at the sediment–water interface. There, slow reacting Fe(III) minerals that have accumulated have a much longer time period for reaction. The large ΣS^{-II} deficit at the interface (Fig. 1) confirms reduction of oxidative particles at the interface.

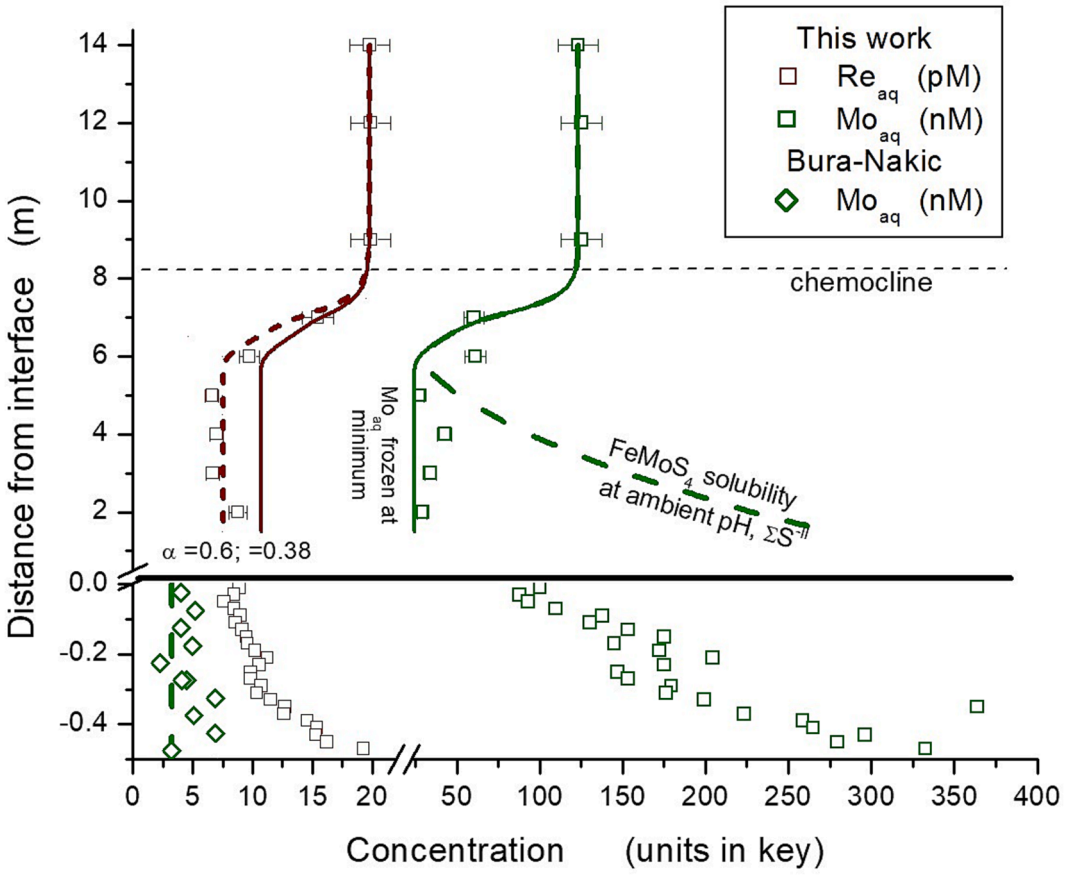

Fig. 6. Detailed comparison of Re_{aq} and Mo_{aq}. Symbols: observed concentrations of Re_{aq} and Mo_{aq} in Rogoznica's water column and pore waters. Curves: calculated concentrations assuming saturation with $Fe(Mo,Re)S_4$ and nanoparticulate FeS ($Q_{FeS} = 10^{4.87}$). Dashed green curve: solubility controlled by ambient pH and ΣS^{-II} at each depth in the water column. Solid green curve: Mo_{aq} profile if Mo is not restored to the aqueous phase at depths deeper than the solubility minimum. Dashed green curve at lower left: Mo_{aq} solubility at average ΣS^{-II} and pH in pore water. Solid red curve: Re_{aq} profile if controlled by coprecipitation in $Fe(Mo,Re)S_4$, given a partition coefficient of 0.38. Dotted red curve: Re_{aq} profile given an adjusted partition coefficient of 0.6. (For interpretation of the references to colour in this figure legend, the reader is referred to the web version of this article.)

Table 2
Calculated concentrations of Mo_{aq}, the non-ionized form of sulfide (H_2S_{aq}), free tetrathiomolybdate and two Fe-tetrathiomolybate dissolved complexes. Below 7 m in Rogoznica's water column, $MoS_nO_{4-n}^{2-}$ species with $n < 4$ are negligible and have been omitted. Z is the height above the sediment–water interface. Assumed: $Q_{FeS} = 10^{4.87}$ in microniches where $Fe(Mo,Re)S_4$ precipitates (see Helz, 2022, for description of the model).

Z (m)	Smoothed ΣS^{-II} (μM)	Smoothed pH	Measured Mo_{aq} (nM)	Calculated Mo_{aq} (nM)	→ H_2S_{aq} (μM)	MoS_4^{2-} (nM)	$[FeO(OH)MoS_4]^{3-}$ (nM)	$[(Fe_2S_2)(MoS_4)_2]^{4-}$ (nM)
Rogoznica	*water*							
9	0.10	8.240	125	≫ 355	0.002			
8	135	7.951		355.6	5.7	2.92	262	4.3
7	428	7.662	60.3	63.9	34.2	4.61	35.1	10.8
6	878	7.324	61.2	24.5*	144	4.05	3.4	8.3
5	1480	7.294	27.7	50.3	259	6.34	2.7	20.5
3	3170	7.234	34.0	153	618	11.68	1.9	69.5
2	4250	7.204	29.1	225	886	14.34	1.5	105
Rogoznica	*Pore water*							
Averages†	1100	6.85	4.6 ± 1.8‡	3.6	435	1.41	0.13	1.01
Malo Jezero	*Pore water*							
−0.25	0.021	7.56	148	159	2.1	0.2	17.6	0.01

* Solubility minimum; below the horizon of this minimum, calculated Mo_{aq} rises but observed Mo_{aq} does not (Fig. 6).
† Owing to scatter in the data, average values of ΣS^{-II} and pH at Z = 0 to −0.63 were used for Rogoznica pore waters.
‡ Measured by Bura-Nakić et al. (2018).

The last row in Table 2 shows calculated Mo speciation at −0.25 m depth in Malo Jezero sediments. Owing to ΣS^{-II} of only 21 μmol/L, H_2S_{aq} is too low to drive appreciable thiolation of MoO_4^{2-} to MoS_4^{2-} and Fe-Mo-S dimers are negligible. The calculated solubility of $Fe(Mo,Re)S_4$ is high enough for Mo_{aq} from reduction of Fe(III) and Mn(III,IV) oxyhydroxides to accumulate to values higher than in seawater before saturation is reached. The measured Mo_{aq} value of 148 nM in Table 2 shows that this actually happens in Malo Jezero's mildly sulfidic pore waters.

Turning attention to the Re data in Fig. 6, the solid red curve traces Re_{aq} concentrations calculated from the Rayleigh distillation law (Eq. (2), assuming coprecipitation of Re_{aq} with Mo_{aq} in $Fe(Mo,Re)S_4$. The

fraction of Mo remaining in solution is taken from the solid green curve representing Mo_{aq} and the partition coefficient (α) is assigned a value of 0.38 (Helz and Dolor, 2012). The calculated Re_{aq} solid curve conforms only qualitatively to the data; it reaches an asymptote that is about 50% too large. The discrepancy might be pointing to an additional Re scavenging mechanism in sulfidic waters, but more likely is indicating that α = 0.38, which was obtained by fitting Black Sea data (Helz and Dolor, 2012), is inappropriate for Rogoznica's much more sulfidic waters. The ReO_4^-/ReS_4^- switch point occurs at $H_2S_{aq} \approx 10^{-3}$ M (Helz and Dolor, 2012), a value reached in Rogoznica's deep waters but not in the Black Sea's. If we adjust the value of α to about 0.6, a reasonably good fit to the Re_{aq} data is obtained (dotted curve, Fig. 6). A higher α in more sulfidic water would imply, plausibly, that Fe(Mo,Re)S_4 is more receptive to Re when it is presented as ReS_4^- than when it is presented as ReO_4^-. Clarifying whether α in natural waters truly varies, and if so by how much, remains a task for the future.

4.3. Re_{auth} and Mo_{auth} in precipitates

The preceding section compared predictions of the Fe(Mo,Re)S_4 coprecipitation model to the composition of Rogoznica's aqueous phase. Now we compare the model's predictions to the compositions of particles both in the water column's suspended material and in sediments.

If irreversible coprecipitation of Mo and Re in Fe(Mo,Re)S_4 were the correct and only mechanism that produces authigenic Mo_s and Re_s in sulfidic basins, then Rogoznica's cumulative $[Re_{auth}/Mo_{auth}]$ ratio in suspended particles and in sediments ought to be predictable from the Rayleigh distillation law (Eq. (3)). Taking $[Re_{aq}/Mo_{aq}]^0_{sw} = 0.415$ from oxic zone data and $f = 0.24$ from Mo_{aq} data in the asymptote region between 2 and 6 m (Fig. 6), we calculate cumulative $[Re_{auth}/Mo_{auth}]_{sw} = 0.31$ if α = 0.6. In this interval, our suspended particle data, corrected for a small lithogenic contribution having Terra Rossa composition (line 8, Table 1), gives $[Re_{auth}/Mo_{auth}]_{sw} = 0.36$ (n = 5, σ = 0.08). Agreement between actual and predicted ratios in suspended particles is quite good.

Difficulty in testing the coprecipitation model against the sediment composition arises because both $[Re_{aq}/Mo_{aq}]^0_{sw}$ and f vary over time, and sediments aggregate the products of this variation. Nonetheless, it is interesting to compare the composition of Rogoznica sediments to predictions based on historical average $[Re_{aq}/Mo_{aq}]^0_{sw}$ and f values. Twelve Rogoznica Lake Mo_{aq} profiles that were obtained at various seasons are available (Helz et al., 2011a; Bura-Nakić et al., 2018; and this work). In the ensemble, surface water salinity has fluctuated because of variations in rainfall and evaporation, but average salinity-normalized Mo_{aq} concentrations are 106 nM at the surface and 12.1 nM at the bottom, making $f = 0.11$. No prior data for Re_{aq} are available, but because the average salinity-normalized Mo_{aq} at the surface is that of seawater, we will assume that salinity-normalized Re_{aq} at the surface is also that of seawater (40 pM). Consequently, $[Re_{aq}/Mo_{aq}]^0_{sw} = 1.00$.

With these assumptions, the predicted $[Re_{auth}/Mo_{auth}]_{sw}$ in Fe(Mo,Re)S_4 that has accumulated in sediments becomes 0.82 if α = 0.6. This prediction of the time-averaged $[Re_s/Mo_s]_{sw,cum}$ is far >0.16 (n = 24, σ = ±0.02) that is observed in Rogoznica sediments (line 2, Table 1). Compared to the observed suspended sediment and modelled $[Re_{auth}/Mo_{auth}]_{sw}$ ratios, Rogoznica sediments seem to contain too much Mo or too little Re.

Based on comparing Mo/Al and Re/Al ratios of Rogoznica sediments in Table 1 to the corresponding ratios in lithogenic source materials like Terra Rossa soils and upper continental crust, the principal process has been addition of Mo, not loss of Re. Rogoznica sediments possess both higher Mo/Al and higher Re/Al than lithogenic sources, but the relative gain in Mo/Al is far larger.

The simplest hypothesis for why the $[Re/Mo]_{sw}$ prediction fails in sediments while it succeeds in suspended particles is that over longer time periods sporadic processes supply additional Mo_{auth} to sediments. Water column mixing during Autumn overturns is such a sporadic process. As surface waters cool, the density profile becomes vertical and the whole water column homogenizes; O_2 and MoO_4^{2-} mix with ΣS^{-II} and Fe^{II}. Initially, the mixed water column is often mildly sulfidic, indicating that reducing equivalents in the hypolimnion slightly exceed oxidizing equivalents in the epilimnion, but whole-lake mixing soon oxygenates the entire water column (Barić et al., 2003). As this process plays out, all the Fe^{II} and Mn^{II} initially stored in the hypolimnion will be converted to ferromanganese oxyhydroxides, which are efficient scavengers of Mo_{aq} but not Re_{aq}.

A potential problem with this hypothesis is that marine ferromanganese precipitates normally have $\delta^{98}Mo$ values ≈−0.7, whereas Rogoznica sediments have $\delta^{98}Mo \approx +1.95 \pm 0.17$ (1σ, n = 13; Fig. 5B). However, this problem can be dismissed if scavenging of Mo_{aq} is nearly complete during overturns. In that case, mass balance constraints would require ferromanganese precipitates to have $\delta^{98}Mo$ approaching seawater's value of +2.37. Unfortunately, water column data collected during an overturn event are not available to test this supposition.

4.4. Ferrothiomolybdate colloids

In Rogoznica Lake pore waters, Bura-Nakić et al. (2018) reported Mo_{aq} concentrations 50-fold smaller than observed by us. The earlier data are plotted as diamond symbols in the lower left corner of Fig. 6. Near the bottom of Table 2, our solubility model has been used to calculate Mo_{aq} at the average pH and ΣS^{-II} *that we observed* in pore waters. As shown by the vertical dashed line at lower left in Fig. 6, the model predicts the solubilities observed by Bura-Nakić et al. (2018) quite well, but underpredicts solubilities we observed by 50-fold. (The calculated Mo_{aq} is much smaller in pore waters than in overlying waters because pH drops from 7.20 to as low as 6.33 across the sediment–water interface, and pH mainly determines the Mo_{aq} asymptote concentration; Helz, 2021). The large underprediction of our measured Mo_{aq} values based on our measured pH and ΣS^{-II} in pore waters requires an explanation.

As indicated above, we suspect that our Mo_{aq} values are much higher than predictions and previous measurements because of our filtration procedure. Bura-Nakić et al., used 0.15 μm Rhizon filters whereas we used 0.45 μm filters. We suggest that some Mo_{aq} is released from particles in shallow sediments in the form of colloids that are able to pass 0.45 μm filters. The colloids appear to contain Re as well as Mo, because over the range of dissolved Mo and Re found in the pore waters, the $(Re_{aq}/Mo_{aq})_{sw}$ ratio is nearly constant at 0.17 ± 0.03.

Previously, evidence has been reported for significant concentrations of Mo-bearing colloids in sulfidic natural waters. Studies by Albéric et al. (2000) first showed that colloids are important Mo carriers at Lake Pavin. Thiam et al. (2014) expanded on this work, showing that in Pavin's pH ≈ 6.0 deep waters, where Mo_{aq} asymptote values would fall at sub-nanomolar levels, most Mo_{aq} passes 0.45 μm filters but can be removed by ultrafiltration. These findings in studies separated by 14 years suggest that colloids have been a continual, not transient, feature of Lake Pavin's deep waters. Similarly, in marine lake Etive, Malcolm (1985) found 1800 nM Mo_{aq} in pore waters (17 times seawater's Mo_{aq}). Most of this occurred in a non-labile form that unlike MoO_4^{2-} was inaccessible to extraction by Chelex resin. Various other authors have made observations of pore waters highly enriched in Mo_{aq} compared to overlying seawater (Morford et al., 2009; Glass et al., 2014; Sulu-Gambari et al., 2017). Failure of these high concentrations to dissipate by diffusion suggests that they are due to colloids, which have diffusion coefficients orders of magnitude smaller than free ions (Schäfer et al., 2012).

Ferrothiomolybdate colloids are well known and sometimes troublesome in laboratory experiments (Vorlicek et al., 2018). They precipitate from Fe^{2+}-MoS_4^{2-} mixtures that are supersaturated with $FeMoS_4$ but can be avoided in MoS_4^{2-} solutions into which Fe^{2+} is introduced by slowly dissolving a low-solubility FeS phase like pyrrhotite (Helz et al., 2014). Their stability may depend on availability of zero-valent sulfur. A fusion sealed glass ampoule charged with pyrrhotite, rhombic sulfur, 1

mM sulfide and 3 μM MoS_4^{2-} solution in University of Maryland laboratories in 2002 still retains the inky black sol that soon formed spontaneously. After more than two decades, the suspension displays no tendency to crystallize, coagulate or sorb to the glass vessel.

Colloids are probably a more important aspect of Mo geochemistry than has been recognized. In the laboratory, formation of homo- and hetero-polyoxomolybdate colloids by acidification of MoO_4^{2-} solutions is well-known (reviewed by Gumerova and Rompel, 2020). Examples of these materials in nature include the amorphous minerals, ilsemannite and ferrimolybdite (Müller et al., 1999; Mekala et al., 2013). The amorphous mineral jordisite may be an example of a colloidal ferro-thiomolybdate material (Vorlicek et al., 2018). Additionally, evidence is accumulating for the importance of Fe-S colloids in sulfidic natural waters (Bura-Nakic et al., 2009b; Helz et al., 2011b). Research on the compositions and structures of all these materials is needed. Their behavior during sediment compaction and diagenesis is so far unknown.

4.5. Oxic zone losses of U_{aq} and Re_{aq}

In those shallower Malo Jezero sediment samples that were deposited under the current, oxic regime, $[Re_s/Mo_s]_{sw}$ ratios are much higher than in upper continental crust and higher even than in Terra Rossa soils (Fig. 5A). The highest $[Re_{aq}/Mo_{aq}]_{sw}$ values, which are in reasonably good agreement with other oxic basin sediments (compare lines 10 and 11 in Table 1), require an authigenic mechanism that deposits mainly Re. Helz (2022) proposes that a Re-specialist mechanism might involve deposition of metastable carbonate phases or of organic particles that have been enriched in Re by iodine-fixing biochemical mechanisms, as originally suggested by Scadden (1969; also see van Sande et al., 2003). Co-enrichment of organic matter in I and Re to the exclusion of related elements like Br and Mo is known in some marine organisms, including brown macroalgae (e.g. kelp, sargassum) and proteinaceous corals.

Our current data do not test definitively either of these proposals. Nonetheless, if we assume that Sr_s in sediments is a proxy for authigenic $CaCO_3$, particularly aragonite, then we should expect a positive correlation between Re_s and Sr_s in sediments if carbonates are scavenging Re. In fact, the correlations are negative in both lakes (Fig. S-3, Supplementary Material). Additionally, Fig. 7 reveals a large U_{aq} peak, but no Re_{aq} peak, just below the sediment water interface in Rogoznica Lake. Lower pH in pore waters compared to bottom waters may be driving dissolution of carbonates, which are known U_{aq} scavengers. If this is the correct explanation for the U_{aq} peak, then the absence of a corresponding Re_{aq} peak raises doubt about carbonate scavenging of Re.

Too little is yet known about the marine biology of Re to fully evaluate the hypothesis that Re is scavenged from oxic waters by biochemical mechanisms. In the Chilika Lagoon, this process has been endorsed by Danish et al. (2021), who attribute 40% of Re scavenging to it. A potential Re-scavenger in the Croatian lakes is the brown alga, *Fucus virsoides,* which historically has been a dominant benthic macrophyte on the rocky shorelines of the Northern Adriatic region (Munda, 1993). It is known to concentrate Re 100–1000 times relative to upper continental crust (Mas et al., 2005; Racionero-Gómez et al., 2016). A substantial fraction of coastal macroalgal productivity resists microbial degradation, especially in hypoxic water (Pedersen et al., 2021), and can be exported into coastal waters (Santos et al., 2021). Also, *Fucus virsoides* releases an extracellular polysaccharide, fucoidan, which can form particles that persist in the environment for hundreds of years (Buck-Wiese et al., 2023). How much Re is transported and dispersed with such products is unknown. Planktonic organisms, such as diatoms, may also have a role in producing Re-rich particles in the ocean (Wagner et al.,

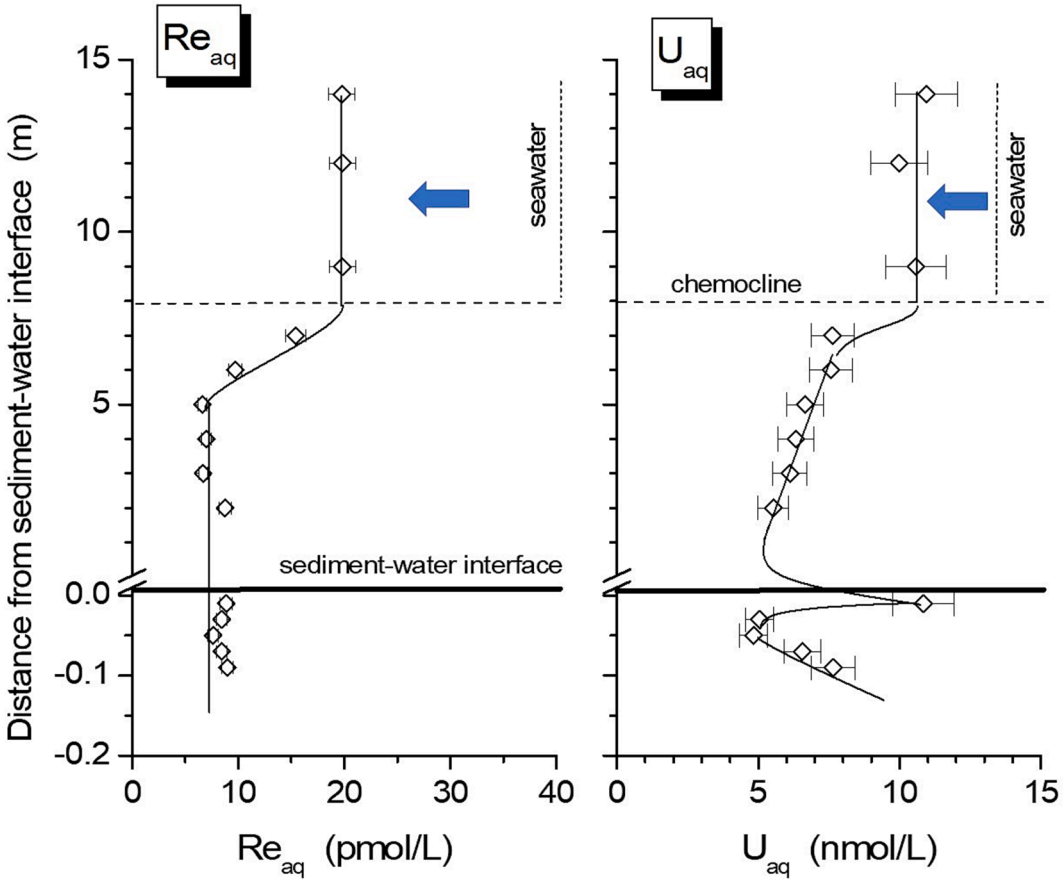

Fig. 7. Linear scale plot of U_{aq} and Re_{aq} data for Rogoznica Lake. Estimated analytical errors are ±10% for U_{aq} and ±6% for Re_{aq} based on duplicate analyses of the same samples.

2013).

In contrast to Malo Jezero, Rogoznica's oxic waters are ≈30% depleted in U_{aq} and ≈50% depleted in Re_{aq} compared to seawater (Fig. 7); Mo_{aq} depletion is negligible (Fig. 4). Re_{aq} depletion suggests that the putative Re-specialist scavenging mechanism is active in Rogoznica's oxic waters. In six water column profiles obtained at various seasons, Bura-Nakić et al. (2018) observed that salinity-normalized U_{aq} in Rogoznica is always depleted relative to seawater while Mo_{aq} is not (no data for Re).

In the ocean, some minor Re_{aq} scavenging from oxic or barely sulfidic waters has been revealed by concentration peaks in shallow marine pore waters (Morford et al., 2009, 2012; Olsen et al., 2017). These peaks, which exceed seawater's concentration, must be sustained by release of Re_{aq} (without Mo_{aq}) from evanescent particles arriving from overlying waters. Data compiled by Bennett and Canfield (2020) also attest to some Re_{aq} scavenging from marine oxic waters; sediments underlying these waters are ≈10-fold enriched in Re_s/Al_s but negligibly enriched in Mo_s/Al_s and U_{aq}/Al relative to continental crust. Despite these lines of evidence, oceanographers find no indication that Mo_{aq}, Re_{aq} and U_{aq} are scavenged from oxic marine water columns (Nameroff et al., 2002; Singh et al., 2011; Goswami et al., 2012, 2022; Ho et al., 2018; Dickson et al., 2020; but see Anbar et al., 1992). The likely explanation for this discrepancy is that lack of observable Re_{aq} depletion in the ocean's oxic surface waters is due to vertical exchange that is rapid enough to replace the scavenged Re_{aq}.

Compared to the ocean, Rogoznica's depletions in Re_{aq} and U_{aq} in the euphotic zone are anomalous, but the lake's shallowness, which situates its oxic water within meters of highly sulfidic water and sediments offers a likely explanation. Vertical exchange cannot replace Re_{aq} and U_{aq} in the surface layer because underlying water is sulfidic and depleted in these elements. Additionally, vertical exchange is inhibited in Rogoznica by its various unique features: its dilution-strengthened density gradient during the wet season, its lack of open exchange with the Adriatic Sea, its small size and its protection from wind by high limestone walls. These all inhibit surface water mixing, enabling oxic-zone Re_{aq} and U_{aq} losses to be observable. Particulate $(Mo/Al)_s$ data (Fig. 4) suggest that limited scavenging of Mo_{aq} in the oxic-zone also occurs but apparently is too feeble to affect Mo_{aq} measurably.

Profiles of U and Re in Fig. 7 differ. In the sulfidic zone, U_{aq} declines linearly to the sediment–water interface whereas Re_{aq} first declines sharply but reaches an asymptote near 6 m. The U_{aq} profile in the sulfidic zone has been discussed by Bura-Nakić et al. (2018), who interpreted the linear gradient as evidence of eddy diffusive transport toward a sink in shallow sediments. The concentration gradient is steeper at the chemocline, which probably indicates that the eddy diffusivity is smaller there owing to a stiffer density gradient. The U_{aq} profile suggests that the loss of U_{aq} from the oxic zone is due primarily to eddy diffusive U_{aq} transport toward the sediments, not scavenging from oxic water.

Complications with this explanation are posed by the large U_{aq} peak that exists at the sediment–water interface and by the upward declining U_{aq} profile in deeper pore waters (Fig. 7). Apparently U_{aq} is diffusing toward a sink at the sediment–water interface from three sources: the water column, shallow sediments, and deeper sediments. The sediment sources attest to two populations of particles that are decomposing and releasing U_{aq} at different rates. The faster-reacting particles, responsible for the shallow peak, may be carbonates, which are known to scavenge U and which would undergo some degree of rapid dissolution in response to the pH drop across the sediment–water interface.

The dominant diffusion flux is the one from the water column. The U_{aq} concentration gradient in the lower water column is $\approx 8.4 \times 10^{-7}$ μg U/cm^4. The eddy diffusion coefficient is roughly 3×10^5 cm^2/yr (Kamyshny et al., 2011; note that eddy diffusivity exceeds molecular diffusivity by five orders of magnitude). These values produce an estimated eddy diffusion flux toward the sediment of 0.3 μg $U_{auth}/cm^2/yr$. The mass accumulation rate of sediment is 0.093 g sed/cm^2/yr (Mihelčić et al., 1996) and our data give the U_{auth} concentration in surface sediments as ≈4 μg U_{auth}/g sed. Thus the mass accumulation rate in sediments is ≈0.4 μg $U_{auth}/cm^2/yr$. The agreement between the calculated eddy diffusion flux and the observed mass accumulation of U_{auth} is surprisingly good given seasonal variations in the concentration gradients and large uncertainties in the eddy diffusion coefficient; this agreement implies that diffusion may be supplying most of the U_{auth} that the sediments receive.

To explain depletion of Re_{aq} from Rogoznica's oxic waters, a similar diffusive mechanism operating across the chemocline might be envisioned. In this case, the sink would occur near the top of the sulfidic water column owing to coprecipitation in $Fe(Mo,Re)S_4$. However, objections to this idea are, first, that Fig. 4 shows distinct enrichment of Re_s on particles within the oxic zone, and second, that the sink in the sulfidic water column fixes both Re_s and Mo_s, but only Re is being measurably withdrawn from the oxic zone. To overcome these objections, we have called upon the same Re-specialist mechanism described above to explain high $[Re_s/Mo_s]_{sw}$ ratios in Malo Jezero sediments.

5. Conclusions

The U behavior in the two Croatian lakes supports previous findings (Bura-Nakić et al., 2018 and references therein) that U is fixed mainly beneath the sediment–water interface in reducing sediments. For Re and Mo, we replace indefinite mechanisms, such as these element's capture by unspecified organic functional groups, their reduction to unspecified products, or their sequential deposition, with a quantitative model postulating coprecipitation in $Fe(Mo,Re)S_4$. The model accounts for the Mo_{aq} and Re_{aq} asymptote pattern that exists in Rogoznica's water column (and widely observed elsewhere in sulfidic waters; Helz, 2021), and it satisfactorily predicts the $[Re_{auth}/Mo_{auth})_{sw}$ ratio in the water column's suspended particles. However, Rogoznica's sediments differ in composition from its suspended particles, and to explain this we must invoke a sporadic contribution from ferromanganese oxyhydroxides. Additionally, to explain the high $[Re_{auth}/Mo_{auth})_{sw}$ ratio in the shallowest Malo Jezero core as well as a 50% depletion of Re_{aq} in Rogoznica's oxic water, we must invoke a formation of Re-rich particles, the nature and origin of which remain unknown. They may be biological, and they probably explain the ≈ 10-fold elevation of Re/Al ratios compared to continental crust in oxic sediments elsewhere (Bennett and Canfield, 2020). The low Al_S in the carbonate-rich sediments of these lakes is responsible for $[E/Al]_S$ ratios that are much higher than in carbonate-poor sediments. Enrichment factors approach values in highly enriched black shales. One consequence is that $[Mo/Al]_S$ and $[U/Al]_S$ ratios misclassify the shallowest Malo Jezero sediments as products of a euxinic basin. Our data demonstrate dramatically the value of $[Re_{auth}/Mo_{auth}]_{sw}$ ratios as redox proxies.

Declaration of Competing Interest

The authors declare that they have no known competing financial interests or personal relationships that could have appeared to influence the work reported in this paper.

Acknowledgements

The authors wish to acknowledge the Croatian Science Foundation (HRZZ-IP-201801-7813) for funding the REDOX project (Geochemistry and redox proxies signature under the diverse environmental conditions: towards better understanding of the past redox) and the Slovenian Research and Innovation Agency (ARIS) for funding the program P1-0143. The authors would also like to thank Jelena Mandić and Tomislav Bulat for their help during sampling, and employees of the National Park Mljet for their assistance. Dario Omanović, Polona Klemenčič and Marta Jagodic Hudobivnik are also acknowledged for their help during analyses.

Appendix A. Supplementary material

Supplementary material includes a PDF file containing an extended comparison of the properties of the two lakes; a comparison of analytical results from this work with published reference values, a side-by-side comparison of the concentrations of Al, Fe, Re, U and Mo in the five cores collected during this work; illustrations of the correlations between Re, U and Mo, as well as the correlations of all three elements with Sr, Ba and Al; and functions used to interpolate pH and ΣS^{-II} data in Rogoznica's water column. A second EXCEL file contains all the data used in this paper. Supplementary material to this article can be found online at https://doi.org/10.1016/j.gca.2023.08.020.

References

Albéric, P., Viollier, E., Jézéquel, D., Grosbois, C., Michard, G., 2000. Interactions between trace elements and dissolved organic matter in the stagnant anoxic deep layer of a meromictic lake. Limnol. Oceanogr. 45, 1088–1096.

Anbar, A.D., Creaser, R.A., Papanastassiou, D.A., Wasserburg, G.J., 1992. Rhenium in seawater: Confirmation of generally conservative behavior. Geochim. Cosmochim. Acta 56, 4099–4103.

Barić, A., Grbec, B., Kušpilić, G., Marasović, I., Ninčević, Ž., Grubelić, I., 2003. Mass mortality event in a small saline lake (Lake Rogoznica) caused by unusual holomictic conditions. Sci. Mar. 67, 129–141.

Bennett, W.W., Canfield, D.E., 2020. Redox-sensitive trace metals as paleoredox proxies: A review and analysis of data from modern sediments. Earth Sci. Rev. 204, 103175.

Benning, L.G., Wilkin, R.T., Barnes, H.L., 2000. Reaction pathways in the Fe-S system below 100 °C. Chem. Geol. 167, 25–51.

Benović, A., Lučić, D., Onofri, V., Peharda, M., Carić, M., Jasprica, N., Bobanović-Colić, S., 2000. Ecological characteristics of the Mljet Island seawater lakes (South Adriatic Sea) with special reference to their resident population of medusae. Sci. Mar. 64, 197–206.

Bone, S.E., Cliff, J., Weaver, K., Takacs, C.J., Roycroft, S., Fendorf, S., Bargar, J.R., 2020. Complexation by organic matter controls uranium mobility in anoxic sediments. Environ. Sci. Tech. 54, 1493–1502.

Buck-Wiese, H., Andskog, M.A., Nguyen, N.P., Bligh, M., Asmala, E., Vidal-Melgosa, S., Liebeke, M., Gustafsson, C., Hehemann, J.-H., 2023. Fucoid brown algae inject fucoidan carbon into the ocean. Proc. Nat. Acad. Sci. 120.

Buljan, M., Špan, J., 1976. Hydrothermal properties of the sea water lakes on the island of Mljet and the adjoining sea in the Eastern South Adriatic Sea. *Acta Adriat.* VI (12), 1–224 (in Croatian).

Bura-Nakić, E., Andersen, M.B., Archer, C., de Souza, G.F., Marguš, M., Vance, D., 2018. Coupled Mo-U abundances and isotopes in a small marine euxinic basin: Constraints on processes in euxinic basins. Geochim. Cosmochim. Acta 222, 212–229.

Bura-Nakic, E., Helz, G.R., Ciglenecki, I., Cosovic, B., 2009a. Reduced sulfur species In a stratified seawater lake (Rogoznica Lake, Croatia); Seasonal variations and argument for organic carriers of reactive sulfur. Geochim. Cosmochim. Acta 73, 3738–3751.

Bura-Nakić, E., Sondi, I., Mikac, N., Andersen, M.B., 2020. Investigating the molybdenum and uranium redox proxies in a modern shallow anoxic carbonate rich marine sediment setting of the Malo Jezero (Mljet Lakes, Adriatic Sea). Chem. Geol. 533, 119441.

Bura-Nakić, E., Knežević, L., Mandić, J., Cindrić, A.-M., Omanović, D., 2021. Rhenium distribution and behavior in the salinity gradient of a highly stratified estuary and pristine riverine waters (The Krka River, Croatia). Arch. Environ. Contam. Toxicol. 81, 564–573.

Bura-Nakic, E., Viollier, E., Jézéquel, D., Thiam, A., Ciglenečki, I., 2009b. Reduced sulfur and iron species in anoxic water column of meromictic crater Lake Pavin (Massif Central, France) Chem. Geol. 266, 311–312.

Čanković, M., Žučko, J., Radić, D., Janeković, I., Petrić, I., Ciglenečki, I., Collins, G., 2019. Microbial diversity and long-term geochemical trends in the euxinic zone of a marine, meromictic lake. System. Appl. Microbiol. 42, 126016.

Chen, I., Walker, R.J., Rudnick, R.L., Gao, S., Gaschnig, R.M., Puchtel, I.S., Tang, M., Hu, Z.-C., 2016. Platinum -group element abundances and Re-Os isotopic systematics of the upper continental crust through time: Evidence from glacial diamictites. Geochim. Cosmochim. Acta 191, 1–16.

Colodner, D., Edmond, J., Boyle, E., 1995. Rhenium in the Black Sea: comparison with molybdenum and uranium. Earth Planet. Sci. Lett. 131, 1–15.

Crusius, J., Calvert, S., Pedersen, T., Sage, D., 1996. Rhenium and molybdenum enrichments in sediments as indicators of oxic, suboxic and sulfidic conditions of deposition. Earth Planet. Sci. Lett. 145, 65–78.

Cuculić, V., Cukrov, N., Kwokal, Ž., Mlakar, M., 2009. Natural and anthropogenic sources of Hg, Cd, Pb, Cu and Zn in seawater and sediment of Mljet National Park, Croatia. *Est. Coast. Shelf Sci.* 81, 211–320.

Dahl, T.W., Chappaz, A., Fitts, J.P., Lyons, T.W., 2013. Molybdenum reduction in a sulfidic lake: Evidence from x-ray absorption fine-structure spectroscopy and implications for the Mo paleoproxy. Geochim. Cosmochim. Acta 103, 213–231.

Danish, M., Tripathy, G.R., Mitra, S., Rout, R.K., Raskar, S., 2021. Non-conservative removal of dissolved rhenium from a coastal lagoon: Clay adsorption versus biological uptake. Chem. Geol. 580, 120378.

Davison, W., 1991. The solubility of iron sulphides in synthetic and natural waters at ambient temperature. Aquatic Sci. 53, 309–321.

Dellinger, M., Hilton, R.G., Nowell, G.M., 2020. Measurements of rhenium isotopic composition in low-abundance samples. J. Anal. At. Spectrom 35, 377–387.

Dickson, A.J., Hsieh, Y.-T., Bryan, A., 2020. the rhenium isotope composition of Atlantic Ocean seawater. Geochim. Cosmochim. Acta 287, 221–228.

Dominovic, I., Dutour-Sikiric, M., Margus, M., Bakran-Petricioli, T., Petricioli, D., Gecek, S., Ciglenecki, I., 2023. Deoxygenation and stratification dynamics in a coastal marine lake. Est. Coast. Shelf Sci. 291, 108420.

Emerson, S.R., Huested, S.S., 1991. Ocean anoxia and the concentrations of molybdenum and vanadium in seawater. Mar. Chem. 34, 177–196.

Faris, J.P., Buchanan, R.F., 1964. Anion exchange characteristics of the elements in nitric acid medium. Anal. Chem. 36, 1157–1158.

Fuller, A.J., Leary, P., Gray, N.D., Davies, H.S., Mosselmans, J.F.W., Cox, F., Robinson, C. H., Pittman, J.K., McCann, C.M., Muir, M., Graham, M.C., Utsunomiya, S., Bower, W. R., Morris, K., Shaw, S., Bots, P., Livens, F.R., Law, G.T.W., 2020. Organic complexation of U(VI) in reducing soils at a natural analogue site: Implications for uranium transport. Chemosphere 254, 126859.

Glass, J.B., Yu, H., Steele, J.A., Dawson, K.A., Sun, S., Chourey, K., Pan, C., Hettich, R.L., Orphan, V.J., 2014. Geochemical, metagenomic and metaproteomic insights into trace metal utilization by methane-oxidizing microbial consortia in sulphidic marine sediments. Environ. Microbiol. 16 (6), 1592–1611.

Goswami, V., Singh, S.K., Ghushan, R., 2012. Dissolved redox sensitive elements, Re, U and Mo in intense denitrification zone of the Arabian Sea. Chem. Geol. 291, 256–268.

Goswami, V., Singh, S.K., Bhushan, R., Rai, V.K., 2022. Spatial distribution of Mo and δ^{98}Mo in waters of the northern Indian Ocean: Role of suboxia and particle-water interactions on lighter Mo in the Bay of Bengal. Geochim. Cosmochim. Acta 324, 174–193.

Gumerova, N., Rompel, A., 2020. Polyoxometalates in solution: speciation under spotlight. Chem. Soc. Rev. 49, 7568–7601.

Hein, J.R., Mizell, K., Koschinsky, A., Conrad, R.A., 2013. Deep-ocean mineral deposits as a source of critical metals for high- and green-technology applications: Comparison with land-based resources. Ore Geol. Rev. 51, 1–14.

Helz, G.R., 2021. Dissolved molybdenum asymptotes in sulfidic waters. Geochem. Perspect. Lett. 19, 23–26.

Helz, G.R., 2022. The Re/Mo redox proxy reconsidered. Geochim. Cosmochim. Acta 317, 507–522.

Helz, G.R., Dolor, M.K., 2012. What regulates rhenium deposition In euxinic basins? Chem. Geol. 304, 131–141.

Helz, G.R., Vorlicek, T.P., 2019. Precipitation of molybdenum from euxinic waters and the role of organic matter. Chem. Geol. 509, 178–193.

Helz, G.R., Bura-Nakic, E., Mikac, N., Ciglenecki, I., 2011a. New model for molybdenum removal from euxinic waters. Chem. Geol. 284, 323–332.

Helz, G.R., Ciglenečki, I., Krznarić, D., Bura-Nakić, E., 2011b. Voltammetry of sulfide nanoparticles and the FeS(aq) problem. In: Tratnyek, P.G., Grundl, T.J., Halderlein, S.B. (Eds.), Aquatic Redox Chemistry, 1071. American Chemical Society Symposium Series, pp. 265–282 (Chap 13).

Helz, G.R., Erickson, B.E., Vorlicek, T.P., 2014. Stabilities of thiomolybdate complexes of iron; implications for retention of essential trace elements (Fe, Cu, Mo) in sulfidic waters. Metallomics 6, 1131–1140.

Ho, P., Lee, J.-M., Heller, M.I., Lam, P.J., Shiller, A.M., 2018. The distribution of dissolved and particulate Mo and V along the U.S. GEOTRACES East Pacific Zonal Transect (GP16): the roles of oxides and biogenic particles in their distributions in the oxygen deficient zone and the hydrothermal plume. Mar. Chem. 201, 242–255.

Hrustić, E., Bobanović-Colić, S., 2017. Hypoxia in deep waters of moderately eutrophic marine lakes, Island of Mljet, eastern Adriatic Sea. Sci. Mar. 81, 431–447.

Imai, N., Terashima, S., Itoh, S., Ando, A., 1999. 1998 compilation of analytical data for five GSJ geochemical reference samples. Geostand. Newslett. 23, 223–250.

Jerden, J.L., Sinha, A.K., 2003. Phosphate based immobilization of uranium in an oxidizing bedrock aquifer. Appl. Geochem. 11, 823–843.

Kamyshny, A., Zerkle, A.L., Mansaray, Z.F., Ciglenečki, I., Bura-Nakić, E., Farquhar, J., Ferdelman, T.G., 2011. Biogeochemical sulfur cycling in the water column of a shallow stratified sea-water lake: Speciation and quadruple sulfur isotope composition. Mar. Chem. 127, 144–154.

Koide, M., Hodge, V.F., Yang, J.S., Stallard, M., Goldberg, E.G., 1986. Some comparative marine chemistries of rhenium, gold, silver and molybdenum. Appl. Geochem. 1, 705–714.

Lin, K., Yang, Z., Yu, T., Ji, W., Liu, X., Li, B., Wu, Z., Li, X., Ma, X., Wang, L., Tang, Q., 2023. Enrichment mechanisms of Mo in soil in the karst region of Guangxi, China. Ecotox. Environ. Saf. 255, 114808.

Malcolm, S.J., 1985. Early diagenesis of molybdenum in estuarine sediments. Mar. Chem. 16, 213–225.

Mas, J.L., Tagami, K., Uchida, S., 2005. Rhenium measurements on North Atlantic seaweed samples by ID-ICP-MS: An observation on the Re concentration factors. J. Radioanal. Nucl. Chem. 265, 361–365.

McDaniel, D.K., Walker, R.J., Hemming, S.R., Horan, M.F., Becker, H., Gauch, R.I., 2004. Sources of osmium to the modern oceans: New evidence from the 190Pt-186Os system. Geochim. Cosmochim. Acta 68, 1243–1252.

Mekala, R., Supriya, S., Das, S.K., 2013. Fate of giant {Mo72-Fe30}-type polyoxometalate cluster in an aqueous solution at higher temperature: understanding related Keplerate chemistry, from molecule to material. Inorg. Chem. 52, 9708–9710.

Mifka, B., Prtenjak, M.T., Kuzmić, J., Čanković, M., Mateša, S., Ciglenečki, I., 2022. Climatology of dust deposition in the Adriatic Sea; A possible impact on marine production. J. Geophys. Res. Atmos. 127, e2021JD035783.

Mihelčić, G., Surija, B., Juračić, M., Barišić, D., Branica, M., 1996. History of the accumulation of trace metals in sediments of the saline Rogoznica Lake (Croatia). Sci. Total Environ. 182, 105–115.

Mikutta, C., Langner, P., Bargar, J.R., Kretzschmar, R., 2016. Tetra- and hexavalent uranium forms bidentate-mononuclear complexes with particulate organic matter in a naturally uranium-enriched peatland. Environ. Sci. Tech. 50, 10465–10475.
Morford, J.L., Emerson, S.R., Breckel, E.J., Kim, S.H., 2005. Diagenesis of oxyanions (V, U, Re, and Mo) in pore waters and sediments from a continental margin. Geochim. Cosmochim. Acta 69, 5021–5032.
Morford, J.L., Martin, W.R., Kalnejais, L.H., François, R., Bothner, M., Karle, I., 2007. Insights on geochemical cycling of U, Re and Mo from seasonal sampling in Bostron Harbor, Massachusetts, USA. Geochim. Cosmochim. Acta 71, 895–915.
Morford, J.L., Martin, W.R., François, R., Carney, C.M., 2009. A model for uranium, rhenium, and molybdenum diagenesis in marine sediments based on results from coastal locations. Geochim. Cosmochim. Acta 73, 2938–2960.
Morford, J.L., Martin, W.R., Carney, C.M., 2012. Rhenium geochemical cycling: Insights from continental margins. Chem. Geol. 324, 73–86.
Mucci, A., 2004. The behavior of mixed Ca-Mn carbonates in water and seawater: Controls of manganese concentrations in marine pore waters. Aquatic Geochem. 10, 139–169.
Müller, A., Sarkar, S., Shah, S.Q.N., Bögge, H., Schmidtmann, M., Sarkar, S., Kögerler, P., Hauptfleisch, B., Trautwein, A.X., Schünemann, V., 1999. Archimedean synthesis and magic numbers: Sizing giant molybdenum-oxide-based molecular spheres of the Keplerate type. Angew. Chem. Int. Ed. Engl. 38, 3238–3241.
Munda, I.M., 1993. Changes and degradation of seaweed stands in the Northern Adriatic. Hydrobiol. 260, 239–253.
Nameroff, T.J., Balistrieri, L.S., Murray, J.W., 2002. Suboxic trace metal geochemistry in the eastern tropical North Pacific. Geochim. Cosmochim. Acta 66, 1139–1158.
Olsen, L., Quinn, K.A., Siebecker, M.G., Luther III, G.W., Hastings, D., Morford, J.L., 2017. Trace metal diagenesis in sulfidic sediments: Insights from Chesapeake Bay. Chem. Geol. 452, 47–59.
Pedersen, M.F., Filbee-Dexter, K., Frisk, N.L., Sárossy, Z., Wernberg, T., 2021. Carbon sequestration potential increased by incomplete anaerobic decomposition of kelp detritus. Mar. Ecol. Prog. Ser. 660, 53–67.
Phillips, R., Xu, J., 2021. A critical review of molybdenum sequestration mechanisms under euxinic conditions: Implications for the precision of molybdenum paleoredox proxies. Earth Sci. Rev. 221, 103799.
Piper, D.Z., Isaacs, C.M., 1995. Minor elements in Quaternary sediment from the Sea of Japan: A record of surface-water productivity and intermediate-water redox conditions. Geol. Soc. Amer. Bull. 107, 54–67.
Pjevac, P., Dyksma, S., Golhammer, T., Mujakić, I., Kobilizek, M., Mussmann, M., Amann, R., Orlić, S., 2019. *In situ* abundance and carbon fixation activity of distinct anoxygenic phototrophs in the stratified seawater lake Rogoznica. Environ. Microbiol. 21, 3896–3908.
Poulton, S.W., Krom, M.D., Raiswell, R., 2004. A revised scheme for the reactivity of iron (oxyhyr)oxide minerals towards dissolved sulfide Geochim. Cosmochim. Acta 68, 3703–3715.
Racionero-Gómez, B., Sproson, A.D., Selby, D., Gröcke, D.R., Redden, H., Greenwell, H. C., 2016. Rhenium uptake and distribution in phaeophyceae macroalgae, *Fucus vesiculosus*. *R. Soc. Open Sci.* 3, 160161.
Razum, I., Bajo, P., Brunović, D., Ilijanić, N., Hasan, O., Röhl, U., Miko, M.S., Miko, S., 2021. Past climate variations recorded in needle-like aragonites correlate with organic carbon burial efficiency as revealed by lake sedimehts in Coratia. Nature Sci. Rept. 11, 7568.
Rolison, J.M., Stirling, C.H., Middag, R., Rijkenberg, M.J.A., 2017. Uranium stable isotope fractionation in the Black Sea: Modern calibration of the 238U/235U paleo-redox proxy. Geochim. Cosmochim. Acta 203, 69–88.
Santos, I.R., Burdige, D.J., Jennerjahn, T.C., Bouillon, S., Cabral, A., Serrano, O., Wernberg, T., Filbee-Dexter, K., Guimond, J.A., Tamborski, J.J., 2021. The renaissance of Odum's outwelling hypothesis in 'Blue Carbon' science. Est. Coast. Shelf Sci. 255, 107361.
Scadden, E.M., 1969. Rhenium: Its concentration in Pacific Ocean surface waters. Geochim. Cosmochim. Acta 33, 633–637.
Schäfer, T., Huber, F., Seher, H., Missana, T., Alonso, U., Kumke, M., Eidner, S., Claret, F., Enzmann, F., 2012. Nanoparticles and their influence on radionuclide mobility in deep geological formations. Appl. Geochem. 27, 390–403.
Sharp, J.O., Lezama-Pacheco, J.S., Schofield, E.J., Junier, P., Ulrich, K.-E., Chinni, S., Veeramani, H., Margot-Roquier, C., Webb, S.M., Tebo, B.M., Giammar, D.E., Bargar, J.R., Bernier-Latmani, R., 2011. Uranium speciation and stability after reductive immobilization in aquifer sediments. Geochim. Cosmochim. Acta 75, 6497–6510.
Simonović, N., Dominović, I., Marguš, M., Matek, A., Ljubešić, Z., Cigelnečki, I., 2023. Dynamics of organic matter in the changing environment of a stratified marine lake over two decades. Sci. Total Environ. 865, 161076.
Singh, S.P., Kumar, S., Bhushan, R., 2011. Behavior of dissolved redox sensitive elements (U, Mo and Re) in the water column of the Bay of Bengal. Mar. Chem. 126, 76–88.
Smedley, P.L., Kinniburgh, D.G., 2017. Molybdenum in natural waters: a review of the occurrence, distributions and controls. Appl. Geochem. 84, 387–432.
Smrzla, D., Zwicker, J., Bach, W., Feng, D., Himmler, T., Chen, D., Peckmann, J., 2019. The behavior of trace elements in seawater, sedimentary pore water, and their incorporation into carbonate minerals: a review. Facies 65, 41.
Sondi, I., Juračić, M., 2010. Whiting events and the formation of aragonite in Mediterranean karstic marine lakes: new evidence on its biologically induced inorganic origin. Sedimentology 57, 85–95.
Sondi, I., Mikac, N., Vdović, N., Ivanić, M., Frudek, M., 2017. Geochemistry of recent aragonite-rich sediments in Mediterranean karstic marine lakes: Trace elements as pollution and palaeoredox proxies and indicators of authigenic mineral formation. Chemosphere 168, 786–797.
Sulu-Gambari, F., Roepert, A., Jilbert, T., Hagens, M., Meysman, F.J.R., Slomp, C.P., 2017. Molybdenum dynamics in sediments of a seasonally-hypoxic coastal marine basin. Chem. Geol. 466, 627–640.
Surić, M., Juračić, M., Horvatinčić, N., Bronić, I.K., 2005. Late Pleistocene-Holocene sea-level rise and the pattern of coastal karst inundation: records from submerged speleothems along the eastern Adriatic Coast (Croatia) Mar. Geol. 214, 163–175.
Tagami, K., Uchida, S., 2007. Determination of rhenium in manganese nodules by inductively coupled plasma mass spectrometry. J. Radioanal. Nucl. Chem. 273, 147–150.
Thiam, A., Jézéquel, D., Groleau, A., Prévot, F., Lopes, F., Albéric, P., Quiblier, C., Bura-Nakić, E., Ciglenečki, I., Lazar, H., Viollier, E., 2014. Biogeochemical dynamics of molybdenum in a crater lake: Seasonal impact and long-term removal. J. Water Resour. Protect. 6, 256–271.
van Sande, J., Massart, C., Beauwens, R., Schoutens, A., Costabliola, S., DuMont, J.E., 2003. Anion selectivity by the sodium iodide symporter. Endochrinology 144, 247–252.
Vlahović, I., Tišljar, J., Velić, I., Matičec, D., 2005. Evolution of the Adriatic carbonate platform; palaegeography, main events and depositional dynamics. Palaegeogr. Palaeoclim. Palaeoecol. 220, 333–360.
Vorlicek, T.P., Helz, G.R., Chappaz, A., Vue, P., Vezina, A., Hunter, W., 2018. Molybdenum burial mechanism in sulfidic sediments; iron-sulfide pathway. ACS Earth Space Chem. 2, 565–576.
Wagner, M., Hendy, I.L., McKay, J.L., Pedersen, T.F., 2013. Influence of biological productivity on silver and redox-sensitive trace metal accumulation in Southern Ocean surface sediments, Pacific sector. *Earth Planet. Sci. Lett.* 380, 31–40.
Wolthers, M., Charlet, L., van der Linde, P.R., Rikard, D., van der Weijden, C.H., 2005. Surface chemistry of disordered mackinawite (FeS). Geochim. Cosmochim. Acta 69, 3469–3481.
Wunsam, S., Schmidt, R., Müller, J., 1999. Holocene lake development of two Dalmatian lagoons (Malo and Veliko Jezero, Isle of Mljet) in respect to changes in Adriatic sea level and climate. Palaeogeogr. Palaeoclim. Palaeoecol. 146, 251–281.
Yamashita, Y., Yoshio, T., Haba, H., Enomoto, S., Shimizu, H., 2007. Comparison of reductive accumulation of Re and Os in seawater-sediment systems. Geochim. Cosmochim. Acta 71, 3458–3475.